# CVD synthesis of nitrogen doped carbon nanotubes using iron pentacarbonyl as catalyst


***By***

***Nafise Ghadimi***


**Submitted in fulfillment of the requirements for the degree of Masters of Science in the Faculty of Science**


**Department of Chemistry**

**University of the Witwatersrand**

**Private Bag X03**

**WITS**

**2050**

**Supervisor: Professor Neil. J. Coville**


**August 2011**

# DECLARATION

I declare that this is my own unaided work under the supervision of Professor Neil. J. Coville. It is being submitted to the Faculty of Science at the University of the Witwatersrand for the degree of Masters of Science. It has not been submitted for any degree or examination in any other University.

Name: Nafise Ghadimi

Signature of candidate …….

……day of…….2011

# DEDICATION

*Lovingly dedicated to my magnificent parents and my supportive sister Hadise*

# ACKNOWLEGMENTS

*I would like to express my gratitude to my Almighty God for his support, kindness, strength, and giving me a supportive family.*

*I would like to thank my supervisor Professor Neil. J. Coville for his infinite support and assistance and also for giving me enough confidence to run this project.*

*I also want to express my great appreciation to my beloved sister Hadiseh and my fantastic parents. Without their support I would not have achieved this stage in my life.*

*I would like to thank, Zikhona, Messai, and Ahmed for their consultation and Manoko and George for doing TGA analysis.*

*I am also thankful to Mr. Rudolph Erasmus for doing Raman analysis.*

*I am also thankful to the Microscopy and Microanalysis Unit, in particular Professor Michael Witcomb, Professor Alexander Ziegler, Caroline Lalkhan and Abe Seema for their assistance.*

*The financial support for this work by the DST/NRF centre of excellence in strong materials is highly appreciated.*

# ABSTRACT

In this dissertation, the synthesis of nitrogen doped carbon nanotubes (N-CNTs) was performed successfully, using a floating catalyst chemical vapour deposition (CVD) method. $Fe(CO)_5$ was utilized as the catalyst and acetonitrile and toluene as nitrogen and carbon sources respectively. Two different procedures were used to add reagents to the reactor: an injection method and a bubbling method. The effect of nitrogen concentration and physical parameters such as reaction temperature, gas flow rate on the morphology, crystallinity and thermal stability of the tubes was studied. The synthesized materials were characterized by means of Raman spectroscopy, TGA and TEM analyses. The presence of nitrogen was confirmed by the presence of the bamboo formations in the tubes by TEM. A comparison of the data from the numerous reactions revealed that N-CNTs can be made from $Fe(CO)_5$ and acetonitrile. Further the main conclusions achieved using the injection method were: i) the maximum number of tubes with bamboo structure were made using on acetonitrile concentration of 15%, ii) The best growth temperature to make N-CNTs was 850 $^{o}$C, iii) An increase in acetonitrile concentration decreased the yield of N-CNTs and iv) Tubes with the narrowest outer diameters were made using an acetonitrile concentration of 15%.

# TABLE OF CONTENTS

# LIST OF FIGURES

# LIST OF TABLES

# LIST OF ABBREVIATIONS

| | |
|---|---|
| SCNM(s) | Shaped carbon nanomaterial(s) |
| CNT(s) | Carbon nanotube(s) |
| N-CNT(s) | Nitrogen doped carbon nanotube(s) |
| CVD | Chemical vapour deposition |
| TGA | Thermal gravimetric analysis |
| TEM | Transmission electron microscopy |
| XPS | X-ray photoelectron spectroscopy |
| SWCNT(s) | Single walled carbon nanotube(s) |
| DWCNT(s) | Double walled carbon nanotube(s) |
| MWCNT(s) | Multi walled carbon nanotube(s) |
| PVD | Physical vapour deposition |
| AACVD | Aerosol assisted chemical vapour deposition |
| DLICVD | Direct liquid injection chemical vapour deposition |
| MPCVD | Microwave plasma assisted chemical vapour deposition |
| ORR | Oxygen reduction reaction |
| ODH | Oxidative dehydrogenation |
| $I_D/I_G$ | The intensity ratio of the D to G band (Raman peaks) |
| CCD camera | Charge coupled device camera |

# CHAPTER 1

## 1. INTRODUCTION

### 1.1 Background to the study

A majority of inventions at the nano scale, that have been described, arise from research in academic and government laboratories. This includes both their discovery and their product development. Nanotechnology products can be found in any field, for example, they can be used in building materials and also in biological materials. Nanomaterials can be used in scratch resistance artefacts and catalysts. They have also been added to polymers to give stronger lighter polymer nanocomposites.

The study of a shaped carbon nanomaterial (SCNM) such as a carbon nanotube is a hot research topic. Many studies were carried out on these types of materials by several researchers during the time period 1952-1989 [1-17]. However it is generally accepted that it is Iijima who brought CNTs to the awareness of the scientific community [18]. He linked their structure to that of fullerenes. CNTs possess many extraordinary properties: they are stronger that steel, harder than diamond, their electrical conductivity is higher than copper and their thermal conductivity is higher than diamond. Consequently, CNTs have become a material, of much interest today. Although there has been much progress in the synthesis of CNT over the years, many challenges still remain in their development. For example, methods to produce CNTs in high purity with controlled morphology, the actual mechanism of carbon growth, and the influence of defects on these physical properties are issues that are still open to study and debate.

Due to the remarkable properties associated with CNTs, scientists have devised strategies to both understand and more importantly to improve on these properties. For example, in 1994 Stephen et al. doped CNTs with N and B atoms using an arc discharge method [19]. Doping not only modified the CNT morphology, but also

changed their electronic properties of the CNTs [20]. The development (synthesis study) of doped CNTs, in particular with nitrogen, is described in **chapter 2**.

Among the techniques, used to make CNTs, the CVD method has been proven to be the most popular and widely used because of its low cost, high production yield and it is an easy method to scale-up. In this dissertation a CVD method was used to make nitrogen doped CNTs (N-CNTs) using a floating catalyst process. In the floating catalyst method both catalyst and carbon source are introduced in the gaseous phase. The method requires a volatile catalyst. Organometallic complexes such as ferrocene (FcH) and substituted ferrocene are typically used. Many studies have been done using ferrocene since the first reports on its first use in 1985 by Komatsu and Endo to fabricate nano shaped materials. But other readily available iron containing organometallic complexes have been used to make CNTs, one of them is iron pentacarbonyl ($Fe(CO)_5$). To date only a few reports exist on the use of $Fe(CO)_5$ to make CNTs, even though it is used commonly in the HiPco process for CNT synthesis. In this dissertation N containing carbon sources have been used in the presence of $Fe(CO)_5$ for the synthesis of N-CNTs. The growth of the N-CNTs was carried out in a tubular furnace in a horizontal quartz tube. The quartz tube was heated (typically 900-1200 $^{o}$C) in the presence of $Fe(CO)_5$ and nitrogen containing compounds by a carrier gas at a controlled flow rate using one of the two methods: (the bubbling and the injection methods). The black soot material formed in the reaction (i.e. the N-CNT containing material) was characterized by transmission electron microscopy (TEM), Raman spectroscopy, and thermogravimetric analysis (TGA).

### 1.2 Objectives

The objectives of this project are as follows:

(i) To synthesis N-doped CNTs by floating catalyst and injection methods using $Fe(CO)_5$ as catalyst. The N source will be nitrogen containing reagents such as acetonitrile.

(ii) To analyse the effect of gas flow rate, temperature and N concentration on N-CNT yield and quality.

(iii) To determine the most productive conditions for N-CNT synthesis using the above methods.

(iv) To characterize the synthesized N-CNTS using Raman spectroscopy, TEM, and TGA analyses procedures.

### 1.3 Outline of the dissertation

Below is an outline of the content of this dissertation:

**Chapter 1:** This chapter gives a review of the motivation for this study and the objectives of the project.

**Chapter 2**: This chapter gives a review of the literature related to carbon nanomaterials such as carbon nanotubes. The structure, physical and chemical properties, synthetic methods, purification procedures and applications of CNTs and in particular N-CNTS will be discussed.

**Chapter 3:** This chapter describes the procedures used to make the N-CNTs. The chapter contains information on the experiments performed and the characterization procedures used to evaluate the yield and quality of the N-CNTs produced. The results are discussed in terms of mechanisms.

**Chapter 4:** In this chapter, conclusions are summarized based on the results obtained with respect to initial objectives. It also includes some recommendation for future studies.

## 1.4 References


1. L. V. Radushkevich, V. M. Lukyanovich, J. Phys. Chem., **1952**, 26, 88.

2. P.A. Tenser, I. Echeistova, D. A. Nauk, USSR, **1952**, 87, 1029.

3. W. R. Davis, R. J. Slawson, G. R. Rigby, Nature, **1953**, 171, 756.

4. L. J. E. Hofer, E. Streling, J. T. McCartney, J. Phys. Chem., **1955**, 59, 1153.

5. P. L. Walker, J. F. Rakszawski, G. R. Imperial, J. Phys. Chem., **1959**, 63, 133.

6. T. Baird, J. R. Fryer, B. Grant, Nature, **1971**, 223, 329.

7. T. Baird, J. R. Fryer, B. Grant, Carbon, **1974**, 12, 591.

8. R. T. K. Baker, M. A. Barber, P. S. Harris, F. S. Feates, R. J. Waite, J. Catalysis, **1972**, 26, 51.

9. R. T. K. Bake, P. S. Harris, R. B. Thomas, R. J. Wiate, J. Catalysis, **1973**, 30, 86.

10. R. T. Baker, R. J. Waite, J. Catalysis, **1975**, 37, 101.

11. T. Koyama, M. Endo, Y. Onuma, J. Appl. Phys., **1972**, 11, 445.

12. A. Oberlin, M. Endo, T. Koyama, J. Cryst. Growth, **1976**, 32, 335.

13. R. T. K. Bake, P. S. Harris, Chemistry and Physics of Carbon, **1978**, 14, 83.

14. R. T. K. Baker, Carbon, **1989**, 27, 315.

15. M. Endo, Chem. Tech, **1988**, 18, 568.

16. M. S. Dresselhaus, G. Dresselhaus, K. Sugihara. I. L. Spain, H. A. Goldberg, Graphite Fibers and Filaments, Springer, Berlin, Germany, **1988.**

17. J. S. Speck, M. Endo, M. S. Dresselhaus, J. Cryst. Growth, **1989**, 94, 834.

18. S. Iijima, T. Ichihashi, Nature, **1993**, 363, 603.

19. O. Stephen, P.M. Ajayan, C. Colliex, Ph Redlich, J.M. Lambert, P. Beirnier, P. Letin, Science, **1994**, 266, 1683.

20. E. N. Nxumalo, N. J. Coville, Materials, **2010**, 3, 2141.

# CHAPTER 2

## 2. LITERATURE REVIEW

### 2.1 Carbon nanomaterials

Carbon is the chemical element with atomic number 6 and symbol C. Carbon is placed in group 14 in the periodic table. Thus carbon is a nonmetallic element. It contains 4 electrons in its valence shell, to form covalent chemical bonds. Carbon can either bond to three atoms with $sp^2$ hybridization or bond to 4 other atoms with $sp^3$ hybridization. Sources of carbon can be either organic (oil, coal) or inorganic (dolomites, limestones).

Carbon resists oxidation more significantly when compared to iron, nitrogen, and copper at room temperature. At high temperature, metal oxides form carbon monoxide and metal. An example is shown as below:

$$Fe_3O_4 + 4C_{(s)} \rightarrow 3Fe + 4CO_{(g)}$$

#### 2.1.1 Allotropes of carbon

Carbon allotropes can be found naturally in the form of, graphite, diamond, amorphous carbon, and carbon spheres as shown in **Figure 2.1** [1]. The physical properties of carbon depends on its allotropic form. Under normal pressure, graphite is the thermodynamically stable form of carbon. In graphite, each C atom is bonded trigonally to three others in a plane composed of hexagonal rings, and this gives rise to a two-dimensional network. The forces between each carbon layer are van der Waals forces. Thus graphite has softness and cleaving properties. Electrical conductivity only occurs in the plane of each covalently bonded sheet. Graphite conducts electricity due to the π bond (the π bond forms due to delocalization of one

of the outer electrons of each atom). At higher pressure, carbon forms a more compact structure having a higher density than graphite. This allotrope is called diamond. In the diamond structure each C atom is bonded tetrahedrally to four others and it forms a three-dimensional network. Its hardness is due to the strength of the C-C bonds. In terms of resistance to scratching it is the hardest material known.

Diamond has different characteristics compared to graphite. Thus diamond is transparent and it is hard whereas, graphite is opaque and very soft. In terms of electrical conductivity diamond has a low conductivity in contrast to graphite which is a good conductor. In addition diamond has a high thermal conductivity under normal conditions. Among all the carbon allotropes graphite has the highest thermodynamic stability. Amorphous carbon is completely anisotropic.

### 2.1.2 Fullerene

Buckminsterfullerene $C_{60}$ (fullerene) was first discovered in 1985 by Harold Kroto, James Heath, Sean O'Brien, Robert Curl and Richard Smalley at Rice University [2].

The $C_{60}$ molecule was called a fullerene and named after Buckminster Fuller. He was an American engineer, inventor and designer. One of his well-known inventions was the geodesic dome. A geodesic dome is a spherical shell structure or lattice shell based on a network of great circles lying on the surface of a sphere. Buckminsterfullerene was named due to its resemblance to geodesic spheres.

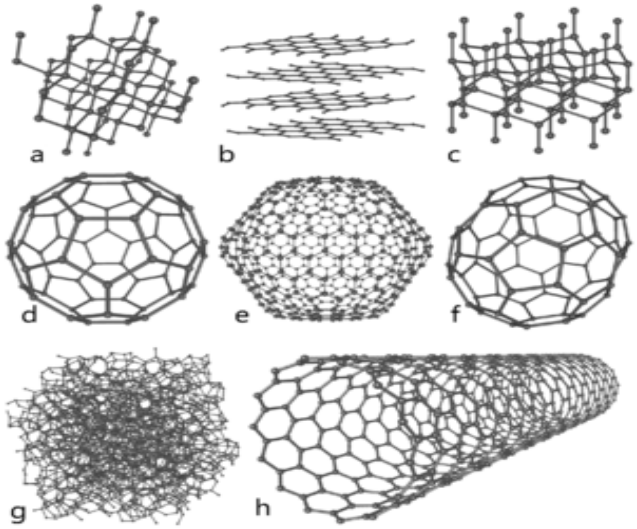


**Figure 2.1:** Some allotropes of carbon: a) diamond; b) graphite; c) lonsdaleite; d, e, f) fullerenes ($C_{60}$, $C_{540}$, $C_{70}$); g) amorphous carbon; h) carbon nanotube [1].

## 2.2 Carbon nanotubes

### 2.2.1 Historical introduction

In 1952 a clear image of a CNT with a 50 nm diameter was published in the Soviet Journal of Physical Chemistry [3]. The discovery remained unknown due to the language that it was published in (Russian). A paper by Orbelin, Endo and Kayama published in 1976 clearly depicted a hollow carbon fiber with a nanometer scale diameter, using a vapour-growth technique [4]. Additionally the authors mentioned that a single layer of graphene was detected from transmission electron microscopy (TEM) images. Later on Endo referred to this image as a single walled nanotube (SWNT). In 1979 the evidence for CNTs was presented at the 14$^{th}$ Biennial conference of Carbon by John Abrahamson. He described CNTs as carbon nanofibers which were produced on carbon anodes during arc discharge. In 1981, carbon nanoparticles were characterized and published by a group of Soviet scientists. They synthesized carbon nanoparticles by the thermocatalytic disproportionation of carbon monoxide. The results from X-ray photoelectron spectroscopy (XPS) and TEM

confirmed that the multilayer tubes were made from carbon atoms. They suggested that their carbon multilayer tubular crystals were formed by rolling graphene layers into cylinders.

In 1987, Tennett of Hyperion Catalysis was issued a U.S patent for the synthesis of cylindrical carbon nanofibres. The carbons had a constant diameter between about 3.5 and about 70 nanometers.

In 1991 Iijima reported that he viewed multilayer CNTs in the insoluble material of arc-discharge graphite rods. This discovery of CNTs accelerated independent discoveries [5,6] by Bethune at IBM [7] and Iijima at NEC of SWCNTs, and methods to synthesis them by adding transition metal-catalysts to the graphite rods in the arc discharge synthesis process.

The discovery of CNTs remains a contentious issue. Many believe it is Iijima who is the discoverer of CNTs because he brought CNTs to the awareness of the scientific community [8], since he linked their structure to that of fullerenes.

### 2.2.2 Structural features of CNTs

Carbon nanotubes (CNTs) are basically allotropes of carbon with a cylindrical structure. The cylindrical structure of CNTs generates novel properties which make them useful in many applications. Individual nanotubes can be applied in electronic devices, such as biosensors, scanning probe tips, sensitive nanobalances etc [9]. As the price of production decreases, the use of macroscopic nanotube derived materials becomes more feasible. Nanotube materials can be available in many forms: e.g. as compressed random mats of raw or purified soot, filter deposited foils [10], spin coated or solvent cast films etc [11]. It is also possible to tailor the physical and chemical properties of CNTs by modifying their structure for use in various applications.

Carbon nanotubes are generally synthesized by the arc evaporation of graphite [12] or by the pyrolysis of hydrocarbons in the presence of metal particles, particularly using

the CVD method [13]. The CVD method is particularly suitable for the synthesis of CNTs in large scale.

### 2.2.3 Types of CNTs

The CNT shape, is based on a plane graphite sheet containing a layer of hexagonal carbons, which shows $sp^2$ hybridizations, that has been rolled into a tube **Figure 2.2** [14].

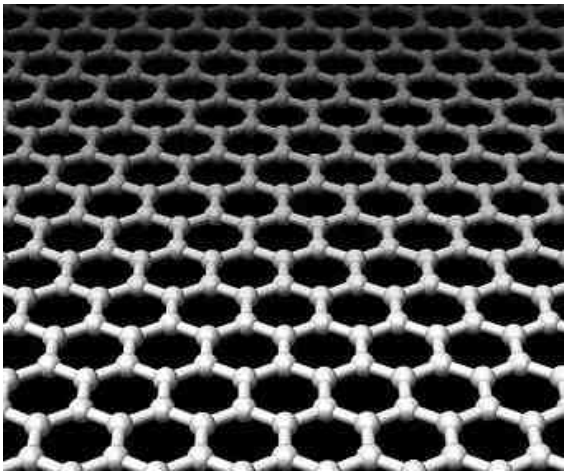

**Figure 2.2:** The structure of graphite [14].

There are generally three types of CNTs have been made **Figure 2.3** [15].

(a) Single-walled carbon nanotubes (SWCNTs): SWCNTs have remarkable properties. But SWCNTs are difficult to synthesize in large yield and in high purity.

(b) Double-walled carbon nanotubes (DWCNTs): DWCNTs consist of two rolled layers of graphite.

(c) Multi-walled carbon nanotubes (MWCNTs): MWCNTs consist of multiple rolled layers of CNTs.

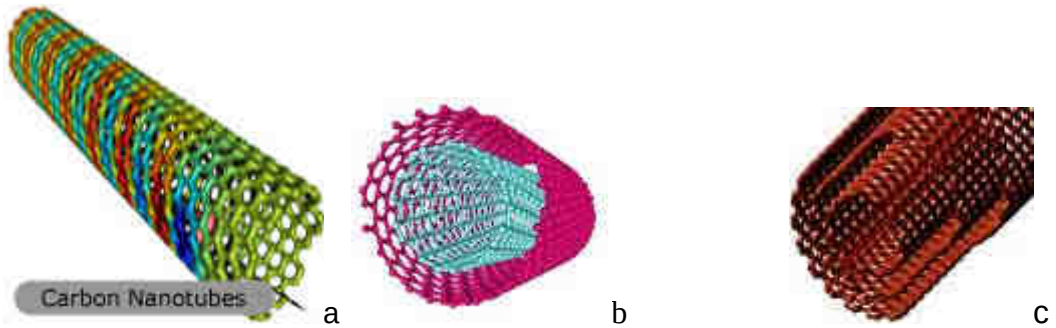


**Figure 2.3:** The different shapes of CNTs. (a) SWCNT, (b) DWCNT, (c) MWCNT [15].

### 2.2.4 Properties of CNTs

CNTs have attracted the attention of scientists due to their remarkable properties. Some examples are given below:

#### 2.2.4.1 Mechanical properties of CNTs

Mechanical properties of bulk materials at the macro level can be transposed directly to the nano level via scaling effects.

What gives CNTs their high stiffness and strength? The strength is due to the strength and adaptability of the C-C bonds. The stiffness is due to the phenomenon of hybridization of a C-C bond in hexagonal carbon rings. In graphite the C atoms are all $sp^2$ hybridized. In CNTs, the curvature is due to a blend of $sp^2$ and $sp^3$ hybridization states in the hexagonal C atoms. When the carbon atoms are under stress they can accommodate the stress by increasing bond angles by assuming more $sp^3$ character. Once the stress is removed, recovery to the original configuration occurs [16].

**(a) Stress:** Stress is the measurement of an average force (F) applied per area ($F.m^{-2}$) The unit of stress is defined as the Pascal (usually associated with Tera, giga, nano units). There are several types of stress: tensile, sheer, compressive and bending.

**(b) Young's modulus:** Young's modulus is the measurement of stiffness. A Young's modulus is a numerical evaluation of Hook's law, i.e. the ratio of stress over strain. In other words it is the measurement of resistance to elastic deformation. Young's modulus is used to determine the length that a material stretches under tension or the load that will make a material buckle under compression. Some examples are depicted in **Table 2.1** [17].

**Table 2.1:** Corresponds to Young's modulus of some materials [17].

| General engineering material | Example | Young's modulus (GPa) |
|---|---|---|
| Metal | Steel<br>Cu<br>Al | 200<br>115<br>69 |
| Carbon materials | Diamond<br>Graphite<br>Single walled CNTs | 1100<br>1100<br>1000+ |
| polymers | Epoxy<br>Polyester<br>Nylon | 6.9<br>6.9<br>3-7 |
| Fibers | C-glass<br>Graphite fiber<br>Boron filament | 69<br>340-380<br>410 |

**(c) Elastic modulus of carbon nanotubes**

Basically, the theoretical Young's modulus of CNTs is predicted to be in the range from 1 to 5 TPa, whereas the best stainless steel and Kevlar values range from 200 and 250 GPa. Respectively, SWCNTs show a ca. 24% elongation of the material at

breaking as compared to 2% for Kevlar and 50% maximum for steel. The high value of a SWCNT Young's modulus correlates with the SWCNT density. Because CNTs have a low density, 1.3-1.4 $g.cm^{-3}$, the specific strength of CNTs can be as high as 4.8 $N.m.kg^{-1}$ much greater than that of high carbon steel (1.3-1.4 $N.m.kg^{-1}$ ).

### 2.2.4.2 Thermal properties

**(a) Coefficient of thermal expansion**: the coefficient of thermal expansion can be explained as a change in the dimension of a material in response to a change in temperature. Carbon nanomaterials normally are characterised by a low co-efficient of thermal expansion. Carbon is used in space craft manufacture where the carbon materials are exposed to temperature extremes [18].

**(b) Thermal conductivity:** thermal conductivity is the ability of a material to conduct heat. The thermal conductivity of CNTs is in the range of 1800-6000 ($W.m^{1}.K^{-1}$) which is 10 times more than that of stainless steel [19].

**(c) Electronic properties:** An electronic property is the ability of a material to conduct electricity. CNTs can in theory be both metallic and semiconducting. Metallic nanotubes can carry an electrical density of $4 \times 10^{9}$ $A/cm^{-2}$ which is 1000 times greater than that of metals e.g. copper [20].

### 2.2.4.3 Chemical properties

Nanomaterials have a high surface energy, thus they seek stabilization by many methods. Some nanomaterials, such as SWCNTs are kinetically stable under room temperature conditions. The graphene structure determines the chemical properties of CNTs.

### 2.2.4.4 Graphite structure

#### (a) Graphite 3D system

Graphite can be defined as an infinite 3D crystal made of several stacked layers with $sp^2$ hybrididzation. Each layer interacts weakly via van der Waals forces.

#### (b) Graphene 2D system

A graphene crystal is an infinite two-dimensional layer consisting of $sp^2$ hybridized carbon atoms. Highly crystalline graphene surfaces usually react with other molecules via physical adsorption ($\pi$-$\pi$ interactions). However, some functional groups such as carboxyl (COOH), amines ($NH_2$), carbonyl (CO) can be anchored at the edges of graphene sheets, which are more the chemically reactive sites. Furthermore, chemical reactivity depends on the termination of carbon at the edges which can either have a zigzag or armchair arrangement. On the other hand to make a graphene surface more reactive, doping with heteroatoms or addition of a high amount of defects or a high degree of curvature is needed.

### 2.2.4.5 Doping of graphene

Doping-induced defects, arising from the introduction of a foreign atom into the graphene sheet is also possible. Doping occurs via substitution of heteroatoms (e.g. N, B) for C atoms. Addition of both dopants increases the chemical reactivity of the graphene surface. Insertion of N adds an extra electron to the surface. The type of defect influences the kind of conduction generated ranging from n-type transport (N substitutional doping) to p-type conduction (substitution of boron atoms into the lattice) [21]. Studies have shown that other elements like Si, P, S can also be introduced into the hexagonal lattice of carbon tubules [22-26].
In summary, the insertion of non-carbon atoms into graphene-like materials can tailor the chemical reactivity and electronic transport of the carbons.

### 2.2.4.6 Physical properties

#### a) Chirality of CNTs

There are generally three different ways to roll graphite sheets to generate a tube. Some of the formed CNTs have mirror symmetry both parallel and perpendicular to the nanotube axis (zigzag and armchair configuration). The other type of CNT is a chiral nanotube which does not have any mirror symmetry. It is shown in **Figure 2.4** [27].

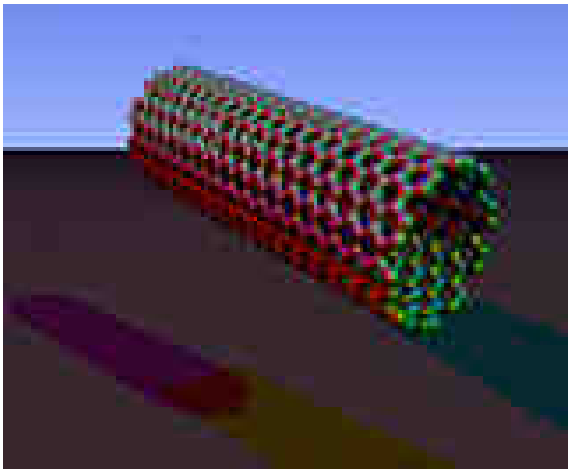

Armchair(n,n)

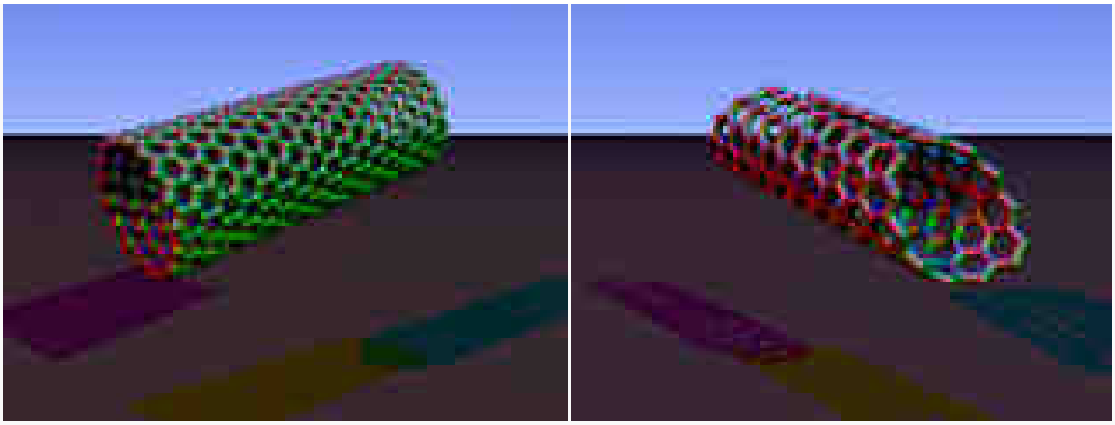

Zigzag (n,0) Chiral (n,m)

**Figure 2.4:** The different shapes of single walled carbon nanotubes [27].

### 2.2.5 Synthesis methods to make CNTs

#### 2.2.5.1 Synthesis methods to make SWCNTs

There are a range of methods that have been developed to make SWCNTs. One of them is the HiPco process. It is a high pressure method that uses CO as a carbon source. Large scale SWCNT synthesis is possible by using this method [28].

HiPco is a gas phase CVD process operating at 30-50 atm and 900-1100 $^{o}$C. The carbon source material used is carbon monoxide and iron pentacarbonyl is the catalyst precursor material. Fe clusters are formed in situ from decomposition of the $Fe(CO)_5$ above 300 $^{o}$C. Condensation of the reduced iron occurs in the gas stream. CO decomposes as shown below:

$2CO \rightarrow CO_2 + C_{swcnt}$

The SWCNTs can be produced with a purity of 97-mol% SWCNTs and contain 3-mol% Fe [28]. The standard reported production conditions are: 30 atm, 1050 $^{o}$C, CO volume flow rate at 8.4 $L.min^{-1}$ and 0.25 torr $Fe(CO)_5$ at 1.4 - 8.4 $L.min^{-1}$ for 24-72 h. The rate of production of SWNTs under these conditions is ca.10.8 $g.day^{-1}$ [28] .

#### 2.2.5.2 Synthesis methods to make MWCNTs

There are several ways in which MWCNTs can be synthesized.

**(a) Arc discharge:** Arc discharge entails the use of two carbon electrodes in an evacuated chamber. Current passes through the two rods. Ultimately one of the rods evaporates (the anode) and condenses on the other rod (cathode). Carbon is vaporised from a graphite rod which condenses on the opposite rod (which has opposite charge) [29]. This method is used to mainly make MWCNTs.

**(b) Laser ablation:** Laser ablation entails the vaporization of carbon. During vaporization the substrate material absorbs energy which is delivered by a laser beam.

The absorbed energy is converted into thermal energy. When evaporation occurs carbon soot will form [30]. Pure CNTs can be formed using this process.

**(c) Chemical vapour deposition (CVD):** The CVD method can easily allow scale up. CVD is used to produce high purity, solid materials. It can make both SWCNTs and/or MWCNTs. The CVD approach involves a chemical reaction, contrary to the physical vapour deposition (PVD) process. CVD is used industrially due to its low cost, flexibility and simplicity. CVD also has the ability to produce high purity ceramics, metallic and semi conducting film at high deposition rates. CVD is a versatile and cost effective system for making CNTs, because the feedstock, a hydrocarbon source, can be used in the solid, liquid or gaseous phase. Further, the reaction can be done on various substrates. Thus, the product can be expected to be available as a thin film, powder or thick coating.

Generally the type of CNTs made depends on the synthesis temperature. For instance production of MWCNTs requires lower temperatures (600-900 $^{o}$C) when compared with SWCNT synthesis (900-1200 $^{o}$C).

A drawback of the CVD techniques is that they produce carbons with structural defects. This implies that the structure of the so-called MWCNTs is far from the ideal rolled-up hexagonal carbon ring lattice shown in figures and cartoons.

There are a range of CVD processes that have been used to make CNTs. These include high or low pressure aerosol assisted CVD (AACVD). Here the precursors are transported to the substrate by means of liquid injection. In the direct liquid injection CVD (DLICVD) method, the precursor is a liquid or a solid (which is dissolved in a liquid) and the liquid is injected into a reactor. The precursor vapour is transported to the substrate. A microwave plasma-assisted CVD (MPCVD) procedure has also been used to make CNTs.

There are two generic approaches to the CVD synthesis methodology. The one is to pass the carbon source in the gas phase over a supported catalyst. In the second approach, both the catalyst and carbon source are gaseous. This procedure is called the floating catalyst method. In the second method volatile organometallic catalysts

can be used. The prototype catalysts are ferrocene **Figure 2.5 a** and $Fe(CO)_5$ **Figure 2.5 b** [31].

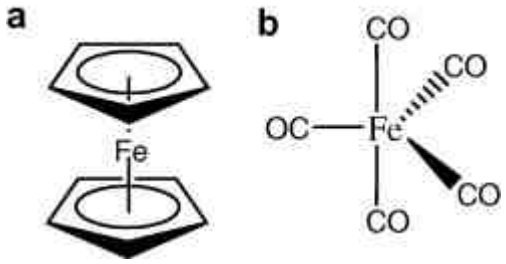


**Figure 2.5:** Catalyst used for CNTs synthesis; (a) ferrocene and (b) $Fe(CO)_5$ [31].

The first use of ferrocene in the synthesis of shaped carbon nanomaterials appeared in 1985 described by Komatsu and Endo [32]. In 1993, a report by Tibbets discribed the use of ferrocene in carbon nanofiber growth [33]. Since then many reports have been written on the use of ferrocene to catalyze carbon shaped nanomaterials from a different range of hydrocarbons.

The factors that make ferrocene popular to apply are; price, accessibility, volatility, and stability in air. Other organometallic catalysts have also been used to make CNTs, but their use has not been as extensively studied. An example is $Fe(CO)_5$.

$Fe(CO)_5$ is used in the HiPco process to produce CNTs [34]. $Fe(CO)_5$ like ferrocene contains Fe and carbon. A major difference is in their oxidation states. $Fe(CO)_5$ has a zero oxidation state whereas, ferrocene formally has the +2 oxidation state. They also differ in their physical states at room temperature: $Fe(CO)_5$ is in a liquid while ferrocene is a solid.

### 2.2.6 CNT purification processes:

CNTs prepared by arc discharge, laser ablation and CVD methods contain many impurities such as amorphous carbon, fullerenes, graphite particles and the metal catalyst. The presence of impurities might affect the performance of CNTs. Hence CNTs must be purified, typically by gas phase oxidation [35-37], liquid phase oxidation [38-44] or physical separation procedures [45-48].

**(a) Gas phase oxidation:** Gas phase oxidation is achieved by the CNTs reacting in air, pure oxygen or chlorine atmospheres at 500 $^{o}$C [36]. Gas oxidative treatments can burn off more than 95% of the nanotube materials [35].

**(b) Liquid phase oxidation:** Liquid phase oxidation can be carried out simply by dipping the sample into strong acids such as concentrated HCl, $HNO_3$ and $H_2SO_4$. To improve this procedure, mixtures of $H_2SO_4$, $HNO_3$ (3:1) or other strong oxidation agent like $KMnO_4$, $HClO_4$ and $H_2O_2$ can be used. Experimental data shows that oxidation of nanotubes in either $HNO_3$ or $H_2SO_4$ is slow. Once a mixture of both is used it improves the yields.

The best oxidation of CNTs is achieved with $KMnO_4$ in an acidic solution. It was demonstrated by Hernadi et al. [41] that oxidation by $KMnO_4$ in a suspension of acid provides nanotubes free of amorphous carbon.

The purification process also opens up the tips of nanotubes leading to the formation of carbonyl and carboxyl groups on the surface of the CNTs. This can improve the dispersion of CNTs in polymers, because such functional group enhances interfacial interaction between the tubes and the polymer [49].

### 2.2.7 Doping of carbon nanotubes

Shaped carbon nanomaterials (SCNMs) have remarkable properties. They are used in the computer industry due to their small size [50-52]. In addition, carbon nanomaterials can be used in catalysis as catalyst support materials or as a catalyst

[53-56]. The range of their applications, can be enhanced by altering their physical-chemical properties. Altering their properties has become a hot topic nowadays. To achieve this goal, SCNMs can be doped by heteroatoms like nitrogen and boron.

Doping is the introduction of a foreign atom into the backbone of a CNT. A CNT doping reaction with N was first reported by Stephen et.al. in 1994 [57]. They doped CNTs with nitrogen using the arc discharge method. The incorporation of nitrogen, with an extra electron compared to carbon, can enhance field emission properties of the carbons [58]. Doping also leads to n-type semiconductor behaviour due to the incorporation of N into CNTs. This leads to an improvement in conductivity [59] and an improvement of field emission properties of CNTs [58]. These improvements are due to the electron donor ability of the nitrogen. For instance, the lone pair on N leads to the presence of an electron in the conduction band and results in n-type semiconduction [60]. When CNTs are doped with N they usually form bamboo compartment in the tube structure and the size of the compartments are a function of the N content. N insertion also causes defects in the walls of the tubes which is desirable in terms of functionalisation. To date, many applications of N-CNTs have been reported such as their use in bio sensors [61], in biological and chemical applications [62-64] and in Li-ion batteries [65].

#### 2.2.7.1 Doping configurations

Incorporation of nitrogen into CNTs can occur in several different bonding configurations, in a graphitic network, as shown in **Figure 2.6** [66]. The three usual bonding configurations are: (a) pyridinic-like $sp^2$ hybridized 6-fold ring arrangement, (b) pyrrolic-like $sp^2$ hybridized 5-fold ring arrangement and (c) a quaternary substitutional, $sp^3$ hybridized 6-fold ring arrangement.

Experimental evidence on the type of N configuration can be achieved via Raman spectroscopy and X-ray photoelectron spectroscopy (XPS). In a Raman spectrum, the prydinic configuration can be confirmed by the intensity ratio of the G to D bands of

N-MWCNTs [69]. From XPS analysis both prydinic and substitutional nitrogen atoms in the hexagonal structure have been revealed [70]. Other configurations can be formed in CNT structures e.g. CN (**Figure 2.7 d**), an amine $NH_2$ (**Figure 2.7 e**), or as $N_2$ intercalated between the graphitic layers[69-72].

Depending on the CNT application, a decision as to which form is most suitable must be made. In the catalytic oxygen reduction reaction (ORR) process, graphitic type N doping showed a better performance compared to others [73,74].

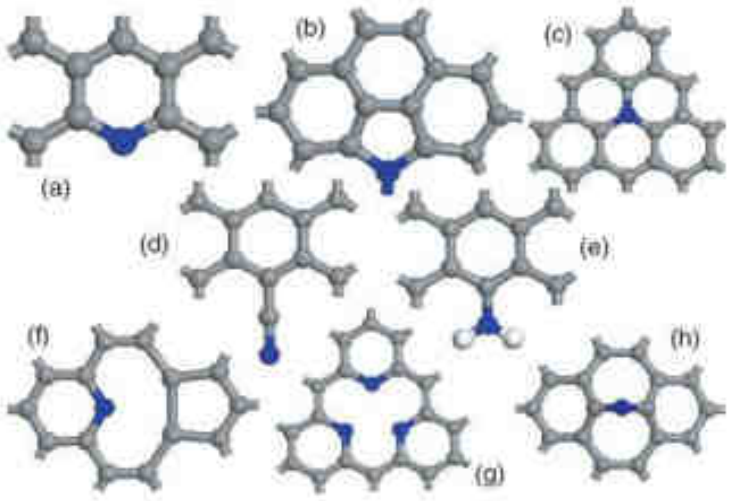


**Figure 2.6:** Possible bonding configurations for N in graphitic networks: (a) pyridine-like N, (b) pyrrole-like N, (c) substitutional N, (d) nitrile - CN, (e) amine - NH2, (f) single N pyridinic vacancy, (g) triple N pyridinic vacancy, and (h) interstitial N [66].

### 2.2.7.2 Defects induced by nitrogen doping

Nitrogen insertion generates defects in the graphitic structure of CNTs. This is shown in **Figure 2.7** [66]: there are vacancies or defects in the lattice **[Figure (2.6 f) or (2.6 g)].** In addition there is a correlation between diameter and type of defect with strain energy induced from curvature of the graphene sheet. Two ranges of diameter have

been studied to provide information on this effect i) a CNT with a diameter less than 8 nm, ii) a CNT with a diameter greater than 8 nm. When a nitrogen defect occurs, the C atoms will move towards the vacancies and form two pentagons sharing the same vertex. For diameters greater than 8 nm, the reconstruction occurs more easily [75].

### 2.2.7.3 N-CNT structure

The structure of N-CNTs have been studied by transmission electron microscopy (TEM). TEM revealed compartmentalized formation within a tube that is referred to as a bamboo structure. This unique morphology associated with the distortion and bending of graphene layers around nitrogen defects, gives a bamboo like structure **Figure 2.7** [76]. It is also proposed, that the outer diameter of undoped CNTs are smaller in diameter when compared to N-CNTs.

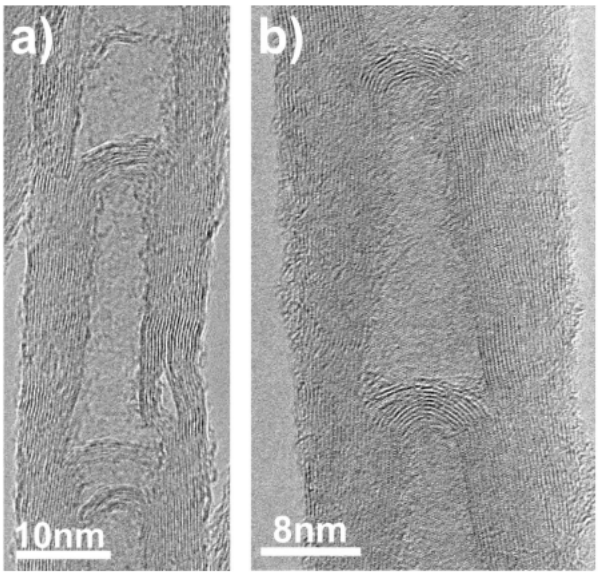


**Figure 2.7:** TEM images of MWCNTS doped with nitrogen, produced by thermolysis of ferrocene-benzylamine solutions at 850 $^{o}$C: (a) low-resolution image of compartmentalized structure of N-CNTs, (b) high-resolution image of an individual bamboo compartment [76].

### 2.2.7.4 Growth mechanism

#### (a) Growth mechanism for undoped CNTs

Undoped MWCNTs consist of several graphene layers that pack around one another. They form a hollow cylindrical structure and terminate by end caps [77]. To satisfy Euler's theorem these caps must include at least six pentagons in a hexagonal network **Figure 2.8** [77].

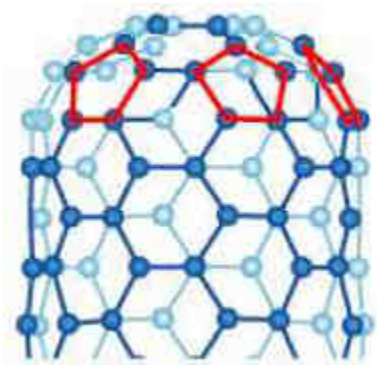

**Figure 2.8:** The position of pentagons in a CNT cap [77].

In some cases, tubes with open ends can be observed. This relates to a sudden growth termination of the tubes due to a sudden change in conditions. These species are unable to form hexagons [78].

A number of studies have been reported on the growth mechanism of CNTs on a supported catalyst [79-94]. Ultimately they all postulate that the mechanism can occur in two different ways: either base or tip growth as shown in **Figure 2.9** [95], depending on the strength of the interaction between catalyst particles and support (metal-support interactions). When a strong interaction exists base growth occurs and vice versa [96]. It is also believed that both mechanisms can occur simultaneously providing both interactions exist in the same catalyst.

In the tip growth mechanism (where the catalyst sits at the tip of CNT) typically the precursor molecules adsorbs on the surface of the catalyst. C atoms are attached to the surface of the catalyst and C atoms can diffuse over the surface. Ultimately C atoms precipitate on the opposite surface to form a CNT wall.

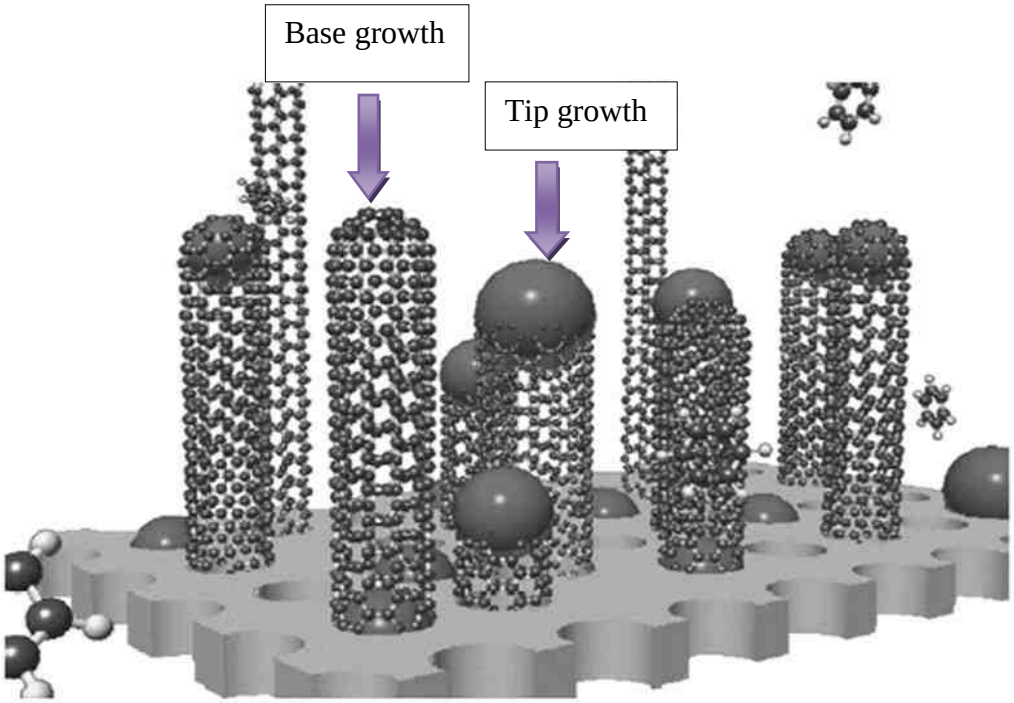


**Figure 2.9:** Schematic of tip and base growth [95].

**(b) Growth of N-CNTs**

To date, a number of mechanistic models for N-CNT growth have been proposed [97]. No conventional nanotube growth models can explain the regular internal bamboo cavities of nitrogen doped MWCNTs. An alternatively growth model proposed for N-doped tubes is shown in **Figure 2.10** [98]. In this method the metal catalyst ejects C and N atoms from the metal particle due to stress accumulated in the

catalyst surface. The formation of the cavities is due to the presence of nitrogen. As the number of layers increases this pressurizes the catalyst particles until material is again ejected from the cavity and the process once gain starts up. This model is supported by the observation that a decrease in the size of catalyst particles decreases the bamboo periodicity [99].

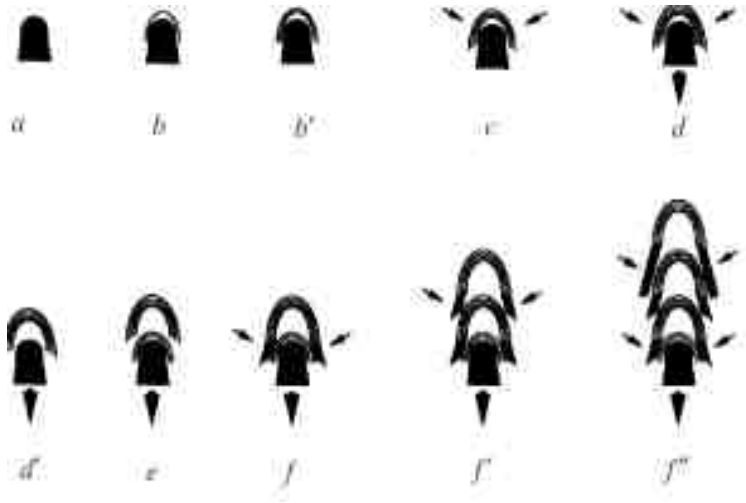

**Figure 2.10:** Growth mechanism proposed for N-doped MCWNT bamboo or 'nanobell' structures. (a) before precipitating carbon layers matching the particle shape (b). The addition of new precipitate layers (b) increases pressure on the catalyst particle (c) until it is ejected from the inside of the cup (d). When the strain is relieved the process can repeatedly (e-f) [98].

### 2.2.7.5 Synthesis of nitrogen doped CNTs

Two synthetic methods have been proposed to make N-CNTs i) insertion of nitrogen into CNTs during the reaction [100-102] and ii) post functionalization of CNTs with nitrogen using organic compounds [103-105]. In the first method, arc discharge [106,107] and laser ablation [102,108] procedures have been used. These techniques

often require a high temperature, typically > 1000 $^{o}$C. An alternative method, which can function at lower temperatures in the presence of an organometallic catalyst and numerous C/N sources is chemical vapour deposition [101,109,110]. The quantity of nitrogen incorporated into the graphene layers of the CNT is challenging. High C/N ratios have been obtained using laser ablation, arc discharge methods and magnetron sputtering (high temperature) techniques (up to 33% N incorporation) [102,106-108,111,112]. Carbons, with up to 20% N incorporation have been achieved with CVD and pyrolysis methods [113-125].

The high temperature techniques to make N-CNTs gives poor quantitative performance compared to these produced by the CVD method [126].

The CVD method can give high yields of both CNTs [127,128] and N-CNTs [129], typically 20-25 g per gram of catalyst.

In the second method N is added to an already made CNT. Thus, the N is deposited on the outer walls of an already made CNT.

Regarding the second method, the major drawback is its complexity due to the multi step synthesis required. To attach an amine group to CNTs requires to be oxidized first. Once it is oxidized it then reacts with amines to obtain N-CNTs.

#### 2.2.7.6 Consequences of N-insertion

Incorporation of nitrogen into CNTs influences the electrical and structural properties of the CNTs. When a CNT is doped with N it generates defects in the graphene layer of the CNTs. The surface is not as smooth as before and attaching other functional groups to CNTs can take place more easily when compared to undoped CNTs. Physical properties of C, N and O atoms are compared in **Table 2.2** [130].

**Table 2.2:** Physical properties of carbon, nitrogen and oxygen [130]. [a]according to Pauling, [b]in aromatic compounds.

| element | Atomic radius (Å) | Electronegativity[a] | C-bond length[b] (Å) | Bond type |
|---|---|---|---|---|
| C | 0.70 | 2.55 | 1.38 | C-C (benzene) |
| N | 0.65 | 3.04 | 1.34 | C-N (pyridine) |
| O | 0.60 | 3.44 | 1.36 | C-O (phenol) |

From **Table 2.2** it can be seen that the bond lengths in aromatic structures containing C-C, C-O and C-N bonds do not differ significantly. The table also indicates that incorporation of N and O atoms in the graphene layers of CNTs is suitable. On the other hand the bond length of a C-N bond is shorter than C-O and C-C bond lengths. The N atom distorts the perfect order in a graphitic matrix. It has also been shown that a low N content (N/C $<$ 0.17) has little effect on a graphene layer and no major change in graphitic properties and morphology of the tube are observed in this case [130].

### 2.2.7.7 CNTs in biological applications

Carbon nanotubes are a useful material to immobilize biomolecules [131]. CNTs can be used in biosensors, drug delivery systems and anti cancer agents, as most biomolecules can adsorbe on CNTs. The great compatibility of CNTs with biomolecules suggested that they can be functionalized with proteins. Each protein can adsorb individually, strongly and noncovalently along the length of CNTs [132]. Proteins such as, ferritin [133-135], cytochrome [136-137] and polysaccharides such as starch [138,139] have been successfully immobilized onto CNTs.

**(a) Functionalisation of N-CNTs with proteins**

N-CNTs possess some distinguishable properties compared to CNTs. For example, they exhibit conductance that is independent of tube chirality [140]. The N doped CNTs are less toxic than CNTs [141], and contain defects which make them provide hydrophobic nitrogen sites [142]. The nitrogen groups can exhibit electron transfer between mettaloproteins and Au electrodes [143-144].

**(b) N-CNTs in biosensing**

The whole potential of N-CNTs for biosensing has not been explored yet. But, it is predicted that the N-CNTs ability to be used will be due to its defects. The nitrogen is distributed inhomogeneously along a tube. Pyridinic nitrogen is useful in terms of binding to incoming species [142-145] and it also creates active sites along the tube wall [146]. In addition it can facilitate the electron transfer between mettaloproteins and an Au electrode.

**2.2.7.8 Role of CNTs and N-CNTs in catalysis**

**(a) Metal supported CNTs**

In general, a good catalyst must possess surface active sites essential for adsorbtion of the reactants, bond breaking, bond formation and desorption of the products. In addition, a catalyst must be sufficiently stable to show efficient catalytic activity over a long period of time. In industry metals and metal oxides are widely used as catalysts.

Nowadays, the availability of new carbon nanomaterials with their peculiar molecular structures and optoelectronic properties, including carbon nanotubes (CNTs), nanodiamonds, graphene sheets and fullerenes offer new ways of developing advanced carbon-based support. To generate metallic catalysts with high catalytic performance [147-150]. Further, it has been shown that the introduction of

heteroatoms (e.g. nitrogen) to carbon nanomaterials leads to electron modulation and this can provide desirable electronic structures for many catalytic processes [147].

There is a report on the use of N-CNTs and N-free CNTs as the support for palladium in the liquid hydrogenation of cinnamaldehyde [151]. It has been reported in this study, that incorporation of nitrogen into the carbon matrix, modified the chemical properties of the support compared to N-free CNTs, leading to a better metal dispersion. The presence of N also significantly improved the selectivity towards the C=C bond in the hydrogenation reaction. Different particle sizes on CNT and N-CNT catalyst supports were observed. Nitrogen atoms on the surface of N-CNTs can provide a surface to increase the anchoring sites on carbon for adsorption of palladium precursor salts. Therefore these anchoring sites could improve the nucleation of the active phase and prevent the metal atom surface mobility resulting in particle sintering during thermal treatments.

Liu et al. [152] have been reported that platinum adsorption was favoured on N-CNT materials compared to the pristine CNTs. They also observed that Pt was adsorbed on those carbons neighboring the N atom. It implies that N atoms did not bond directly to the metal, but the N atoms only acted as donor like atoms and not directly as binding sites for the deposited metal active phase. The nitrogen atoms located inside the carbon network are likely to play an intermediate activator role for the metal adsorption on the carbon site.

In summary, the catalytic behavior of metals has been tested on both CNT and N-CNT supports to evaluate the role of the support on the catalytic activity. The results showed that N-free CNTs demonstrated the lower hydrogenation activity compared to N-CNTs. This could be attributed to different dispersion of the metal particles on the support surfaces.

It is noteworthy, to consider that even the type of N species in the N-CNTs play an important role in catalyst binding and it is believed that graphitic type N-CNTs show the best results [153].

**(b) Metal-free carbon catalysts**

A metal based catalyst suffers from several disadvantages, including high cost, low selectivity, poor durability and detrimental environmental effects caused by catalyst residue and/or undesirable side-products [147]. Thus it is highly desirable to design inexpensive, metal free catalysts that have good activity and high performance over a long period of time. CNTs have been proposed as ideal catalysts for some chemical reactions due to their remarkable properties these include corrosion resistance, environmental acceptability, and unique surface properties. Glassy carbon and activated carbons have been used for certain chemical and electrochemical processes for a long time [154,155]. Carbon-based metal-free catalysts, can be involved in reduction and oxidation reactions [147,156].

In the case of nanostructured carbon nanomaterials (e.g. CNTs) the weakest adsorption sites are associated with the basal planes and consist of the hexagonal arrangement of carbon atoms. The high energy sites exist at the CNT edges and are often saturated with hydrogen atoms that can be replaced by other heteroatoms like, oxygen or nitrogen. These atoms provide strong chemical reactivities for redox or acid-base reactions. A carbon catalyst showed a good potential in ODH reactions of saturated hydrocarbons [157-162]. In particular many carbon nanostructures such as CNTs [159], carbon nanodiamonds [162] and CNFs [159,160] have been found suitable to catalyze the ODH reaction of ethylbenzene to styrene **Figure 2.11** [163]. Some nanocarbon catalysts have demonstrated better catalytic performance and long-term stability when compared with metal oxide catalysts [164].

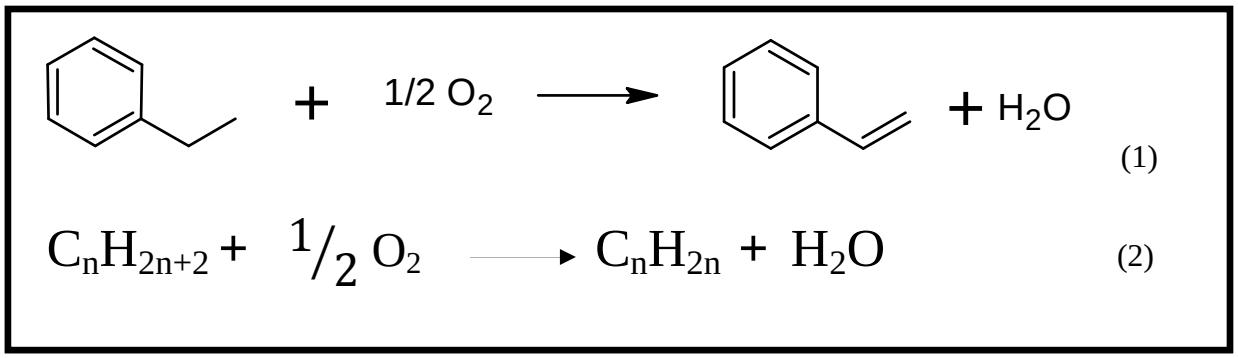


**Figure 2.11:** ODH of ethylbenzene [163].

**(c) CNTs in fuel cells**

Fuel cells convert chemical energy directly to electricity [165]. At the anode, a catalyst oxidizes the fuel, usually hydrogen, generates a positive charge and a negative charge electron. The electrolyte which is placed between the cathode and the anode can let ions pass through it. But electrons pass through the wire and generates an electric current. When the ions reach the cathode they reunite with the electrons and the two react with a third chemical, usually oxygen, to form $H_2O$. The catalyst that is used in this system is Pt. During this process a slow oxygen reduction reaction (ORR) occurrs on the Pt cathode and a large amount of Pt is reduced at the anode, due to $H_2$ oxidation. The ORR occurs in two ways, either through a $4e^-$ process or a less efficient two step $2e^-$ pathway. The Pt-based electrode suffers from its susceptibility to time dependent drift and CO deactivation. Nowadays replacement/reduction of the expensive Pt-based electrodes is under investigation. Some examples include electrocatalysts made from a Pt-based alloy, transition metal chalcogenides, carbon nanotube-supported metal particles etc. [166-168]. The performance of N-CNTs or N-CNFs has demonstrated some good electrocatalytic activity [167]. A synthesized N-CNF electrode prepared by the floating catalyst CVD method using ferrocene, and either xylene or pyridine has demonstrated good electrocatalytic activities for ORR via a two-step two-electron pathway [169]. In addition N-CNF electrodes showed a 100 fold increase in catalytic activities for $H_2O_2$

decomposition under both neutral and alkaline conditions [170]. In a recent report Gong et al. [171] found that vertically aligned N-CNTs could act as efficiently as metal-free ORR electro catalysts in fuel cells.

The metal-free N-CNTs were shown to catalyze a $4e^-$ ORR process free from CO poisoning and with greater electrocatalytic activity and better long-term stability than Pt-based electrodes in alkaline electrolytes **Figure 2.12** [163]. Aligned N-CNTs provides the high surface area, good electrical and mechanical properties and superb thermal stability for the nanotube electrode to be used in fuel cells under either room temperature, or harsher temperature conditions.

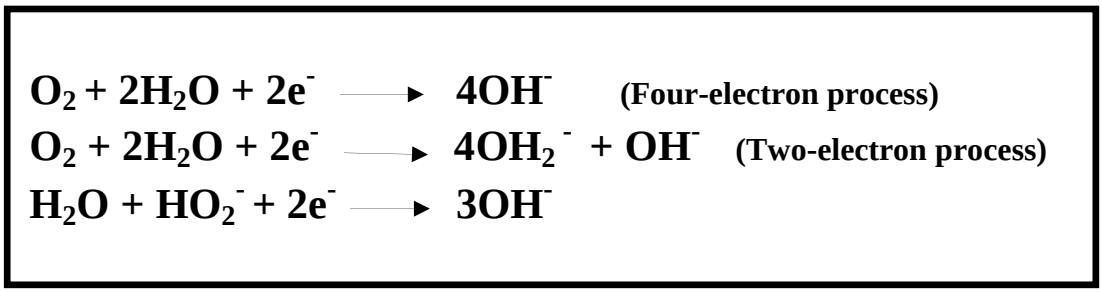


**Figure 2.12:** A 4 $e^-$ ORR process [163].

Gong et al. [171] attributed the improvement of catalytic performance to the electron-accepting ability of the nitrogen atoms. Thus nitrogen forms a net positive charge on adjacent carbon atoms in the nanotube plane of the NCNTs. Hence, nitrogen attracts more electrons from the anode to facilitate the ORR. The nitrogen delocalization changes the chemisorptions of $O_2$ (at the n-free CNT surface) to a side-on adsorption on N-CNT electrodes. However N-induced charge transfer from adjacent carbon atoms might lower the ORR potential and the parallel diatomic adsorption could significantly weaken O-O bonding, facilitating ORR at the vertically aligned N-CNTs electrodes. The discovery of this ORR mechanism has led to the development of various other metal-free efficient ORR catalysts for fuel cell applications.

Furthermore, the role of nitrogen influences the design/development of new catalytic materials for fuel cell and other applications [172-179]. It is noticeable that nitrogen plays an important role as an active site for nanocarbon ORR catalysts and this nitrogen can be found in three different forms (pyrrolic, pyridinc, graphitic). Chen et al. [173] produced N-CNTs from different N-sources using a single step CVD process. They found that N-CNTs with higher nitrogen content and more distortion exhibited better ORR performance in acidic electrolytes. On the other hand Kundu et.al. [174] prepared N-CNTs at different temperatures. They observed, more pyridinic nitrogen at 550 $^{o}$C which showed better ORR electrocatalytic activity that the one prepared at 750 $^{o}$C. This study revealed that more graphitic than pyridinic nitrogen atoms are necessary for the ORR. It is still a challenge to determine the exact location of nitrogen atom in carbon nanotubes.

### 2.2.7.9 Characterization techniques used for carbon nanotubes

#### (a) Transmission electron microscopy

Transmission electron microscopy (TEM) can be used to understand matter at dimensions of roughly 1 to 100 nm. TEM experiments can assist on understanding of carbon in terms of modeling, imaging, measuring and manipulating matter at the nano scale. TEM can be used to analyze, metals, alloys, ceramics, polymers, semiconductors and composite mixture of these materials [180]. TEM operates on the same basic principle as light microscopy. The major difference is an electron is used instead of light. A light microscope is limited due to the wavelength of light. TEM uses electrons with shorter wavelengths. Therefore it is plausible to get a thousand times greater resolution with electron microscopy than using normal light microscopy [181].

The limitations of TEM are, i) interpreting transmission images, TEM represents an image with 2D system obtained from a 3D specimen. One of the problems is that when a 2D image is viewed the image does not reveal depth ii) electron beam damage

of the sample due to ionization. Ionization has a detrimental effect on a specimen and it could damage the sample, particularly polymers. Nowadays one the solutions is to use a minimum energy dose, cooling procedures and, charge coupled device (CCD) cameras [180].

The sample should be electron transparent. It means that the specimen must be thin enough to transmit electrons, until enough electrons can be detected.

**(b) Raman spectroscopy**

Raman spectroscopy is a useful and non-destructive technique. It is widely used to identify the graphitic nature of CNTs. Raman spectroscopy is very sensitive to structural disorder that breaks the graphitic lattice translational symmetry as it measures features in small crystals [182]. It is also sensitive to strength, length and the arrangement of chemical bonds in a sample but less sensitive to chemical composition. A Raman effect arises when a beam of intense monochromic light passes through a sample which contains molecules that change their polarizability as they vibrate. The position of the bands change according to the structures. For CNTs characteristic peaks are found in three spectral regions. The radial breathing mode (RBM) peaks occur around 120-250 $cm^{-1}$ and indicate the diameter of SWNCNTs. The G-band is characterized by peaks around 1580 $cm^{-1}$ and indicates the graphitic nature of CNTs. The D-band peak occurs around 1350 $cm^{-1}$ and corresponds to disorder features in graphitic sheets. The overall quality of a carbon material can be identified by the $I_D/I_G$ ratio, where $I_D$ = intensity of the D band and $I_G$ = intensity of the G band. The higher the $I_D/I_G$ ratio, the lower the graphitic structural quality of the material [183].

**(c) Thermogravimetric analysis**

The TGA technique investigates changes in the weight of a sample as a function of temperature. Such a technique relies on three factors: weight loss, temperature,

temperature change [184]. Typically all weight loss curves look similar. To avoid any misinterpretation, derivative weight loss curves can be used. The derivative curve identifies the exact point at which weight loss is most apparent. From TGA curves, data on the kinetics, thermodynamics of chemical reactions, reaction mechanisms, reaction intermediates and final reaction products are obtained [185]. TGA is used to determine the thermal stability of CNTs. Furthermore the presence of a catalyst residue and the absorbed moisture content in a sample can be checked by TGA.

## 2.3 Toxicity of carbon nanotubes

The toxicity of CNTs remains as a controversial subject and more research is still needed. Due to the great role of CNTs in industry it is vital to consider the health hazards of these new developed materials. It is believed that the needle like fiber shaped CNTs are similar to asbestos fibers. Thus, exposure to CNTs for a long time would cause mesothelima, which is a cancer of the lining of the lungs [186]. But the toxicity of these material depends on parameter data, structure, size distribution, surface area, surface charge and purity of samples. The presented data suggest that under some conditions nanotubes can pass membrane barriers. When raw materials reach the organs they generate some harmful effects e.g. inflammatory and fibrotic reactions [186].

Warheit et al. studied the toxicity of SWCNTs in rats by examining the ability of these nano particles to generate pulmonary inflammation as well as alter lung cellular proliferation [187]. They observed pulmonary granuloma formation following SWCNT exposure. In contrast to quartz particles, SWCNTs resulted in multifocal pulmonary granumola formation without any evidence of ongoing pulmonary inflammation or cellular proliferation. Warheit et al. found that the ability of SWCNTs to cause granulo matus lesions by a unique mechanism within the lung may relate to the unique physicochemical properties of SWCNTs [187]. In addition, the unique structural properties of SWCNTs make them resistant in biological and

ecological systems. The bio-persistancy of SWCNTs may become a significant health safety issue.

## 2.4 Conclusion

This chapter has indicated the background information to the experimental study performed in this dissertation. What is clear from the study is that the use of organometallic floating catalysts to make CNTs has been dominated by the use of ferrocene and its derivatives. Further, while $Fe(CO)_5$ is used in the HiPco process to successfully make CNTs, its use to make N-CNTs has not be studied. Only two reports have appeared in the literature in which $Fe(CO)_5$ and pyridine were used [188,189]. The study that follows is based on the following questions:

1) Can N-CNTs be made using $Fe(CO)_5$ as a floating catalyst and acetonitrile as nitrogen source?

2) If the N-CNTs can be made, can their purity and morphology be controlled?

It is to be noted that this study is a synthesis study. The N-CNTs synthesized have not been used (in this study) as catalyst supports. This will be done in later work.

## 2.5 References

1. www.wikipedia.org/wiki/carbon, 29 May **2011.**

2. H. W. Kroto, J. R. Heath, S. C. O'Brien, R. F. Curl, R. E. Smalley, Nature, **1985**, 318, 162.

3. I. B. Radushkevich, J. Phys. Chem., **1952**, 26, 88.

4. A. Oberlin, J. Cryst. Growth Des., **1976**, 32, 335.

5. D. S. Bethune, C. H. Klang, M.S. de Vries, G. Gorman, R. Savoy, J. Vazquez, R. Beyers, Nature, **1993**, 363, 605.

6. S. Iijima, T. Ichihashi, Nature, **1993**, 363, 603.

7. www.almaden.ibm.com/st/past_projects/nanotubes, 29 May **2011.**

8. M. Monthioux, V. Kuznetsov, Carbon, **2006**, 44, 1621.

9. R. H. Baughman, A. A. Zakhidov, W. A. De Heer, Science, **2002**, 297, 787.

10. A. G. Rinzler, J. Liu, P. Nikolaev, C. B. Huffman, F. J. Rodriguez-Macias**,** P. J. Boul, A. H. Lu, D. Heymann, D. T. Colbert, R. S. Lee, J. E. Fischer, A. M. Rao, P. C. Eklund, R. E. Smallery, J. App. Phys., **1998**, 67,29.

11. T. V. Sreekumar. T. Liu, S. Kumar, L. M. Ericson, R. H. Hauge, R. E. Smalley, Chem. Mater., **2003**, 15, 175.

12. S. Iijima, T. Ichihashi, Nature, **1993**, 363, 603.

13. A. Cassell, J. A. Rraymarkers, J. Kong, H. Dai, J. Phys. Chem., **1999**, 103, 6484.

14. www.wikipedia.org/ Carbon _nano_tubes. 03 March **2010.**

15. www.nano.org.uk/Carbon_nano_tubes. 22 May **2010.**

16. E. W. Wong, P.E. Sheehan, C. M. Lieber, Science, **1997**, 277, 1971.

17. G. L. Hornyak, J. J. Moore, H. F. Tibbals, J. Dutta, Fundamental of nanotechnology, CRC, New York, USA**, 2009** .

18. www.stormcable.com/thermal_ expansion_data_table. 28 February **2010.**

19. J. Hone, M. Whitney, C. Piskoti, A. Zettl, Phys. Rev., **1999**, 59, 2514.

20. A. Bilusic, J. Lukatela, J. Dolinsek, Strojarstvo **2006**, 48, 13.

21. M. S. Dresselhaus, M. Terrones, A. Jorio, M. Endo, A. Rao, Y. Kim, T. Hayashi, H. Terrones, J. Charlier, G. Dresselhaus, Materials today magazine, **2004**, 7, 30.

22. J. Campos-Delgado, I. O. Maciel, D. A. Cullen, D. J. Smith, A. Jorio, M. A. Pimenta, H. Terrones, M. Terrones, ACS. Nano, **2010,** 4, 1696.

23. E. Cruz-Silva, F. López-Urías, E. Mu˜noz-Sandoval, B. G. Sumpter, H. Terrones, J. C. Charlier, V. Meunier, M. Terrones, ACS. Nano, **2009**, 3, 1913.

24. M. Terrones, A. Jorio, I.O. Maciel, J. Campos-Delgado, E. Cruz-Silva, M. A. Pimenta, B. G. Sumpter, V. Meunier, F. López-Urías, E. Mu˜noz-Sandoval, H. Terrones, Nano Lett., **2009,** 9, 2267.

25. J. M. Romo-Herrera, D. A. Cullen, E. Cruz-Silva, D. Ramírez, B. G. Sumpter, V. Meunier, H. Terrones, D. J. Smith, M. Ter-rones, Adv. Funct. Mater, **2009**, 94, 1193.

26. L. Novotny, A. Jorio, I. O. Maciel, N. Anderson, M. A. Pimenta, A. Hartschuh, H. Qian, M. Terrones, H. Terrones, J. Campos-Delgado, A. M. Rao, Nature. Mater., **2008**, 7, 878.

27. www.wikipedia.org/carbon _nano _tubes. 03 March **2010.**

28. M. J. Bronikowski, P. A Willis, D. T. Colbert, K. A. Smith, R. E. Smalley. J. Vac. Sci. Tech., **2001**, 19, 1800.

29. Ph. Redlich, M. J. Loeffler, P. M Ajayan, J. Bill, F. Aldinger. J. Chem. Phys., **1996**, 260, 465.

30. A. Thess, R. Lee, P. Nikolaev, H. J. Dai. Science, **1996**, 273, 483.

31. S. D. Mhlanga, K. C. Mondal, R. Carter, M. J. Witcomb, J. Organo. Chem., **2008**, 693, 2942.

32. Y. Komastsu, M. Endo, Japanese patent 60-32818, **1985**.

33. G. G. Tibbetts, D. W. Gorkiewicz, Carbon, **1993**, 31, 809.

34. P. Nikolaev, M. J. Bronikowski, R. K. Bradly, F. Rohmund, D. T. Colbert, K. A. Smith, R. E. Smalley, Chem. Phys. Lett., **1999**, 313, 91.

35. T. W. Ebbesen, P. M. Ajayan, H. Hiura, K. Tanigaki, Nature, **1994**, 367, 319.

36. J. L. Zimmerman, R. K. Bradley, C. B. Huffman, R. H. Hauge, J. L. Margrave, J. Mater. Chem., **2000**, 12, 1361.

37. Y. S. Park, Y. C. Choi, K. S. Kim, Carbon, **2001**, 39, 655.

38. H. Hiura, T. W. Ebbesen, K. Tanigaki, Advacnced Material, **1995**, 7, 275.

39. A. Rinzler, J. Liu, H. Dai, P. Nikolaev, C. B. Huffman, F.J. Rodriguez, P. J. Boul, D. Heymann, D. T. Colbert, R.S. Lee, E. Fischer, A. M. Rao, P. C. Eklund, R. E. Smalley, J. App. Phys., **1998**, 67, 29.

40. I. W. Chiang, B.E. Brinson, R. E. Smalley, J. Phys. Chem., **2001**, 105, 1157.

41. K. Herandi, A. Siska, L. Thien-Nga, L. Forro, I. Kiricsi, Solid State Ionic, **2001**, 141, 203.

42. C. M. Chen, M. Chen, Y. W. Peng, H. W. Yu, C. F. Chen, Thin Solid Films, **2006**, 498, 202.

43. S. Porro, S. Musso, M. Vinante, L. Vanzetti, M. Anderle, F. Trotta, A. Tagliaferro, Physica, **2007**, 37, 58.

44. C. M. Chen, M. Chen, Y. W. Peng, C.H. Lin, L. W. Chang, C. F. Chen, Diam. Relat. Mater, **2005**, 14, 798.

45. S. Bandow, A. M. Rao, K. A. Williams, A. Thess, R. E. Smalley, P. C. Eklund, J. Phys. Chem, **1999**, 101, 8839

46. K. B. Shelimov, R. O. Esenaliev, A. G. Rinzler, C. B. Huffman, R. E. Smalley Phys. Chem. Lett., **1998**, 282, 429.

47. F. Li, H. M. Cheng, Y. T. Xing, P. H. Tan, G. Su, Carbon, **2000**, 38, 2041.

48. A. Yu, E. Bekyarova, M. E. Itkis, D. Fakhrutdinov, R. Webster, R. C. Haddon, ACS. Nano, **2006**, 128, 9902.

49. S. C. Tjong, Mater. Sci. Eng., **2006**, 53, 73.

50. R. H. Baughman, A. A. Zakhidov, W. A. de Heer, Science, **2002**, 297, 787.

51. P. Avouris, J. Chem. Phys., **2002**, 281, 429.

52. F. Kreupl, A. P. Graham, G. S. Duesberg, W. SteinHögl, M. Liebau, E. Unger, W. Hönlein, Microelectron. Eng., **2002**, 64, 399.

53. K. P. de Jong, J. W. Geus, Catal. Rev. Sci. Eng, **2000**, 42, 481.

54. P. Serp, M. Corrias, P. Kalck, Appl. Catal, **2003**, 253, 337.

55. J. H. Bitter, M. K. van der Lee, A. G. T. Slotboom, A. J. van Dillen, K. P. de Jong, Cat. Let, **2003**, 89, 139.

56. N. Keller, N. I. Maksimova, V. V. Roddatis, M. Schur, G. Mestl, Y. V. Butenko, V. L. Kuznetsov, R. Schlögl, Angew. Chem. Int. Ed, **2002**, 41, 1885.

57. O. Stephen, P.M. Ajayan, C. Colliex, Ph. Redlich, J. M. Lambert, P. Beirnier, P. Letin. Science, **1994**, 266, 1683.

58. R. B. Sharma, D. J. Late, D. S. Joag, A. Govindaraj, C. N. R. Rao, Chem. Phys. Lett., **2006**, 428, 102.

59. D. Golberg, Y. Bando, C. C. Tang, T. E. Zhi, Adv. Mater, **2007**, 19, 2413.

60. M. Terrones, P. M. Ajayan, F. Banhart, X. Blasé, D. L. Carroll, J. C. Charlier, R. Czerw, B. Foley, N. Grobert, R. Kamalakaran, P. Kolhler-Redlich, M. Ruhle, T. Seeger, H. Terrones, J. Appl. Phys., **2002**, 74, 355.

61. P. W. Barone's Baik, D. A. Heller, and M. S. Strano, Nature Materials, **2005**, 4, 86.

62. J. C. Carrero-Sanchez, A. L. Elias, R. Mancilla, G. Arrelin, H. Terrones, J. P. Laclette, M. Terrones, Nano. Lett, **2006**, 6, 1609.

63. A. L. Elias, J. C. TCarrero-Sanchez, H. Terrones, M. Endo, J. P. Laclette, M. Terrones, Small, **2007**, 3, 1723.

64. B. Fragneaud, K. Masenelli-Varlot, A. Gonzalez-Montiel, M. Terrones, J. Cavaille, Chem. Phys. Lett., **2006**, 419, 567.

65. Z. Zhou, X. Gao, J. Yan, D. Song, M. A. Morinaga, Carbon, **2004**, 42, 2677.

66. Y. T. Lee, N. S. Kim, J. Park, J. B. Han, Y. S. Choi, H. Ryu, H. J. Lee, Chem. Phys. Lett., **2003**, 372, 853.

67. J. H. Yang, B. J. Kim, Y. H. Kim, Y. J. Lee, B. H. Ha, Y. S. Shin, S. Y. Park, H. S. Kim, C.Y. Park, C. W. Yang, J. B. Yoo, M. H. Kwon, K. Ihm, H. J. Song, T. H. Kang, H. J. Shin, J. Y. Park, J. M. Kim.J. Vac. Sci. Techol., **2005**, 23, 930.

68. M. Nath, B. C. Satishkumar, A. Govindaraj, C. P. Vinod, C. N. R. Rao, Chem. Phys. Lett., **2000**, 322, 333.

69. M. Reyes, N. Grobert, R. Kamalakaran, T. Seeger, D. Golberg, M. R¨uhle, Y. Bando, H. Terrones, M. Terrones, Chem. Phys. Lett., **2004**, 396, 167.

70. K. Suenaga, M. Yudasaka, C. Colliex, and S. Iijima, Chem. Phys. Lett., **2000**, 316, 365.

71. J. Kotakoski, A. V. Krasheninnikov, Y. Ma, A. S. Foster, K. Nordlund, R. M. Nieminen, Phys. Rev., **2005**, 71, 205408.

72. H. C. Choi, S. Y. Bae, J. Park, K. Seo, C. Kim, B. Kim, H. J. Song, and H. J. Shin, Appl. Phys. Lett., **2004**, 85, 574.

73. R. Liu, D. Wu, X. Feng, K. Mullen, Angew. Chem., Int. Ed, **2010**, 49, 2565.

74. H. Niwa, K. Horiba, Y. Harada, M. Oshima, T. Ikeda, K. Terakura, J. Ozaki, S. Miyata, J. Power. Sources, **2009**, 187, 93.

75. D. Srivastava, M. Menon, C. Daraio, S. Jin, B. Sadanadan, A. M. Rao. Phys. Rev, **2004**, 69, 153414.

76. B. G. Sumpter, V. Meunier, J. M. Romo-Herrera, E. Cruz-Silva, D. A. Cullen, H. Terrones, D. J. Smith, M. Terrones, ACS. Nano, **2007**, 1, 369.

77. D. Zhou, L. Chow, Appl. Phys, **2009**, 93, 9972.

78. S. Iijima, P. M. Ajayan, T. Ichihashi. Phys. Rev. Lett., **1992**, 69, 3101.

79. A. C. Dupuis, P. Mater. Sci, **2005**, 50, 929.

80. H. Liu, D. Takagi, H. Ohno, S. Chiashi, T. Chokan, Y. Homma, J. Appl. Phys., **2008**, 1, 014001.

81. M. Endo, T. Hayashi, Y.A. Kim, M. Terrones, M.S. Dresselhaus, Phil. Trans. Roy. Soc. Lond, **2004**, 362, 2223.

82. R.S. Wagner, W.C. Ellis, Trans. AIME, **1965**, 233, 1053.

83. R.T.K Baker, Carbon, **1989**, 27, 315.

84. H. Kanzow, A. Ding, J. Phys. Rev, **1999**, 60, 11180.

85. Y. Ayumu, K. Noboru, M. Watari, J. Phys. Chem, **2002**, 106, 51.

86. S.B. Sinnot, R. Andrews, D. Qian, A.M. Rao, Z. Mao, E.C. Dickey, F. Derbyshire, Chem. Phys. Lett., **1999**, 315, 25.

87. K. Liu, K. Jiang, C. Feng, Z. Chen, S. Fan, Carbon, **2005**, 43, 2850.

88. R. Seidel, G.S. Duesberg, E. Unger, A.P. Graham, M. Liebau, F. Kreupl, J. Phys. Chem, **2004**, 108, 1888.

89. M. Pérez-Cabero, E. Romeo, C. Royo, A. Monzón, A. Guerrero-Ruíz, I. Rodríguez-Ramos, Catal, **2004**, 224, 197.

90. A. Reina, M. Hofmann, D. Zhu, J. Kong, J. Phys. Chem, **2007**, 111, 7292.

91. C. Jin, K. Suenaga, S. Iijima, ACS. Nano, **2008**, 2, 1275.

92. R. Brukh, S. Mitra, Chem. Phys. Lett., 2006, **424**, 126.

93. M. Grujicic, G. Cao, B. Gersten, Appl. Surf. Sci., **2002**, 191, 223.

94. Y. Homma, Y. Kobayashi, T. Ogino, D. Takagi, R. Ito, Y.J. Jung, P.M. Ajayan, J. Phys. Chem. **2003**, 107, 12161.

95. V. O. Nyamori, S. D. Mhlanga, N. J. Coville, J. Organomet. Chem. **2008**, 693, 2205.

96. http://students.chem.tue.nl/World of Carbon_Nanotube. 18 July **2008.**

97. K. Suenaga, M. Yudasaka, C. Colliex, S. Iijima, Chem. Phys. Lett., 2000, 316, 365.

98. M. Terrones, A. M. Benito, C. Manteca-Diego, W. K. Hsu, O. I. Osman, J. P. Hare, D. G. Reid, H. Terrones, A. K. Cheetham, K. Prassides, H. W. Kroto, D. R. M. Walton, Chem. Phys. Lett. **1996**, 257, 576.

99. S. Trasobares, O. Stéphan, C. Colliex, W. K. Hsu, H. W. Kroto, D. R. M. Walton, J. Chem. Phys. **2002**, 116, 8966.

100**.** M**.** Terrones**,** R. Kamalakarana, T. Seegera, M. Rühlea, M. Rühle, H. W. Kroto, D. R. M. Walton, Adv. Mater., **1999**, 11, 655.

101. H. C. Choi, J. Park, B. Kim, J. Phys. Chem. **2005**, 109, 4333.

102. J. Hu, P. Yang, C. M. Lieber, Phys. Rev. **1998**, 57, 3185.

103. J. Li, M. J. Vergne, E. D. Mowles, W-H Zhong, D. M. Hercules, C. M. Lukehart, Carbon**, 2005**, 43, 2883.

104. E. N. Konyushenko, J. Stejskal, M. Trchova, J. Hradil, J. Kovarova, J. Prokes, M. Cieslar, Polymer, **2006**, 47, 5715.

105. T. Ramanathan, F. T. Fisher, R. S. Ruoff, L. C. Brinson, Chem. Mater. **2005**, 17, 1290.

106. F. Le Normand, J. Hommet, T. Szörényi, C. Fuchs, E. Fogarassy, Phys. Rev., **2001**, 64, 2354161.

107. R. Droppa Jr., P. Hammer, A. C. M. Carvalho, M. C. dos Santos, F. Alvarez, J. Non-Cryst. Solids, **2002**, 299, 874.

108. S. E. Rodil, W. I. Milne, J. Robertson, L. M. Brown, Appl. Phys. Lett., **2000**, 77, 1458.

109. Y. T. Lee, N. S. Kim, J. Park, J. B. Han, Y. S. Choi, H. Ryu, H. J. Lee, Chem. Phys. Lett., **2003**, 372, 853.

110. M. Terrones, A. M. Benito, C. Manteca-Diego, W. K. Hsu, O. I. Osman, J. P. Hare, D. G. Reid, H. Terrones, A. K. Cheetham, K. Prassides, H. W. Kroto, D. R. M. Walton, Chem. Phys. Lett., **1996**, 257, 576.

111. K. Suenaga, M.P. Johansson, N. Hellgren, E. Broitman, L.R. Wallenberg, C. Colliex, J.E. Sundgren, L. Hultman, Chem. Phys. Lett., **1999**, 300, 695.

112. N. Hellgren M. P. Johansson, E. Broitman, L. Hultman, J. E. Sundgren, Phys. Rev., **1999**, 59, 5162.

113. M. He, S. Zhou, J. Zhang, Z. Liu, C. Robinson, J. Phys. Chem., **2005**, 109, 9275.

114. R. Sen, B. C. Satishkumar, A. Govindaraj, K. R. Harikumar, G. Raina Chem. Phys. Lett., **1998**, 287, 671.

115. R. Sen, B. C. Satishkumar, A. Govindaraj, K. R. Harikumar, M. K. Renganathan, C. N. R. Rao, J. Mat. Chem., **1997**, 7, 2335.

116. X. Wang, H. Liu, Q. Zhao, Y. Li, Y. Liu, F. Lu, J. Zhang, S. Wang, L. Jiang, D. Zhu, D. Yu, L. Chi, J. Phys. Chem., **2002**, 106, 2186.

117. M. Glerup, M Glerup, M Castignolles, M Holzinger., Chem. Commun., **2003**, 20, 2542.

118. T. Matsui, M. Yudasaka, R. Kikuchi, Y. Ohki and S. Yoshimura, Appl. Phys. Lett., **1994**, 65, 2145.

119. A. G. Kudashov, A. V. Okotrub, N. F. Yudanov, A. L. Romanenko, L. G. Bulusheva, O. G. Abrosimov, A. L. Chuvilin, E. M. Pazhetnov, J. Phys. Chem., **2004**, 108, 9048.

120. T. Y. Kim, K. R Lee, K. Y. Eun, K. H Oh, Chem. Phys. Lett., **2003**, 372, 603.

121. T. Nakajima, M. Koh, Carbon, **1997**, 35, 203.

122. R. I. Kvon, G. N. Il'nich, A. L. Chuvilin, V. A. Likholobov, J. Molec. J. Mol. Catal., **2000**, 158, 413.

123. Z. Yang, Y. Xia, R. Mokaya, Chem. Mater., **2005**, 17, 4502.

124. S. Trasobares, O. Stephan, C. Colliex, W. K. Hsu, H. W. Kroto, J. Phys. Chem., **2002**, 116, 8966.

125. M. Nath**,** B. C. Satishkumar**,** A. Govindaraj**,** C. P. Vinod**,** C. N. R. Rao**,** Chem. Phys. Lett., **2000**, 322, 333.

126. H. Dai, Surf. Sci., **2002**, 500, 218.

127. M. L. Toebes, J. H. Bitter, A. J. van Dillen, K. P. de Jong, Catal. Today, **2002**, 76, 33.

128. M. K. van der Lee, A. J. van Dillen, J. W. Geus, K. P. de Jong, J. H. Bitter, Carbon, **2006**, 44, 629.

129. C. Tang, Y. Bando, D. Goldberg, F. Xu, Carbon, **2004**, 42, 2625.

130. D. R. Lide, Handbook of Chemistry and Physics 85th edition, CRC, Florida, USA, **2004**,.

131. S. C. Tsang, Z. Guo, Y. K. Chen, M. L. H. Green, H. A. O. Hill, T. W. Hambley, P. J. Sadler. Angew. Chem. Int. Ed., **1997**, 36, 2197.

132. J. J. Davis, K. S, Coleman, B. R Azamian, C. B. Bagshaw, and M. L. H. Green. Chem. Eur. J, **2003**, 9, 3732.

133. R. J. Chen, S. Bangsaruntip, K. A. Drouvalakis, N. Wong Shi Kam, M. Shim, Y. Li, W. Kim, P. J. Utz, and H. Dai. Proc. Natl. Acad. Sci. USA, **2003**, 100, 4984.

134. S. Bhattacharyya, C. Sinturel, J. P. Salvetat, M. L. Saboungi, Appl. Phys. Lett., **2003**, 86, 113104.

135. R. Prakash, R. Superfine, S. Washburn, M. R. Falvo. Appl. Phys. Lett., **2006**, 88, 63102.

136. B. R Azamian, J. J. Davis, K. S. Coleman, C. B. Bagshaw, and M. L. H. Green. J. Am. Chem. Soc., **2002**, 124, 12664.

137. Y. Lin, L. F. Allard, and Y. P. Sun. J. Phys. Chem., **2004**, 108, 3760.

138. A. Star, D. W. Steuerman, J. R. Heath, and J. F. Stoddart. Angew. Chem. Int. Ed., **2002**, 41, 2508.

139. O. K. Kim, J. Je, J. W. Baldwin, S. Kooi, P. E. Pehrsson, and L. J. Buckley. J. Am. Chem. Soc., **2003**, 125, 4426**.**

140. H. J. Burch, J. A. Davies, E. Brown, L. Hao, S. Antoranz Contera, N. Grobert, and J. F. Ryan. Appl. Phys. Lett., **2006**, 89, 143110.

141. J. C. Carrero-S´anchez, A. L. El´ıas, R. Mancilla, G. Arrell´ın, H. Terrones, J. P. Laclette, M. Terrones, Nano Lett., **2006**, 6, 1609.

142. F. Villalpando-P´aez, A. H. Romero, E. Munoz Sandoval, L. M. Mart´ınez, H. Terrones, M. Terrones, Chem. Phys. Lett., **2004**, 386, 134.

143. M. J. Eddowes, H. A. O. Hill, J. Chem. Soc. Chem. Comm., **1977**, 21, 771.

144. F. A. Armstrong, H. A. O. Hill, and N. J. Walton, Acc. Chem. Res., **1988**, 21, 407.

145. S. Peng and K. Cho, Nano Lett., **2003**, 3, 513.

146. C. P. Ewles and M. Glerup, J. Nanosci. Nanotechnol., **2005**, 5, 1345.

147. D. S. Sue, J, Zhang, B, Frank, A. Thomas, X. Wang, J. Paraknowitsch, R. Schlögl, ChemSusChem, **2010**, 3, 169.

148. L. Dai, Carbon Nanotechnology Recent Developments in Chemistry, Physics, Materials Science and Device Applications, Elsevier, Amsterdam, Netherlands, **2006**.

149. J. Wu, W. Pisula, K. Müllen, Chem. Rev., **2007**, 107, 718.

150. M. J. Allen, V. C. Tung, R. B. Kaner, Chem. Rev., **2010**, 110, 132 .

151. K. Chizari, I. Janowska, M. Houllé, I. Florea, O. Ersen, T. Romero, P. Bernhardt, M. J. Ledoux, C. Pham-Huu, Appl. Catal., **2010**, 380, 72.

152. R. Liu, D. Wu, X. Feng, K. Müllen, Angew. Chem., Int. Ed. **2010**, 49, 2565.

153. H. Niwa, K. Horiba, Y. Harada, M. Oshima, T. Ikeda, K. Terakura, J. Ozaki, S. Miyata, J. Power Sources, **2009**, 187, 93.

154. J. Muniz, G. Marban, A. B. Fuertes, Appl. Catal, **2000**, 27, 27.

155. A. Sarapuua, K. Vaika, D. J. Schiffrinb, K. Tammeveski, J. Electroanal. Chem. **2003**, 541, 23.

156. P. R. Schreiner, Chem. Soc. Rev., **2003**, 32, 289.

157. A. Schraut, G. Emig, H.G. Sockel, Appl. Catal., **1987**, 29, 311.

158. D.S. Su, N. Maksimova, J.J. Delgado, N. Keller, G. Mestl, M. J. Ledoux, R. Schlögl, Catal. Today, **2005**, 102, 110.

159. T. J. Zhao, W. Z. Sun, X. Y. Gu, M. Rønning, D. Chen, Y. C. Dai, W. K. Yuan, A. Holmen, Appl. Catal., **2007**, 323, 135.

160. G. Mestl, N. I. Maksimova, N. Keller, V.V. Roddatis, R. Schlögl, Angew. Chem., **2001**, 40, 2066.

161. N. Keller, N.I. IMaksimova, V.V. Roddatis, M. Schur, G. Mestl, Y. V. Butenko, V. L. Kuznetsov, R. Schlögl, Angew. Chem., **2002**, 41, 1885.

162. D. S. Su, N. I. Maksimova, G. Mestl, V. L. Kuznetsov, R. Schlögl, N. Keller, Carbon **2007**, 45, 2145.

163. D. Yu, E. Nagelli, F. Du, L. Dai, Phys. Chem. Lett., **2010**, 1, 2165.

164. J. Zhang, D. A. Sua. Zhang, D.Wang, RC. Hèrbert, Angew. Chem., **2007**, 46, 7319.

165. S. Basu, Recent Trends in Fuel Cell Science and Technology, Anamaya Publishers, New Delhi, India, **2007**.

166. G. Che, B. B. Lakshmi, E. R. Fisher, C. R. Martin, Nature, **1998**, 393, 346.

167. J. Yang, D. Liu, N. N. Kariuki, L. X. Chen, Chem. Commun. **2008**, 3, 329.

168. A. Kongkanand, S. Kuwabata, G. Girishkumar, P. Kamat, Langmuir **2006**, 22, 2392.

169. K. Maldonado, K. J. Stevenson, J. Phys. Chem., **2004**, 108, 11375.

170. S. Maldonado, K.J. Stevenson, J. Phys. Chem., **2005**, 109, 4707.

171. K. Gong, F. Du, Z. Xia, M. Durstock, L. Dai, Science, **2009**, 323, 760.

172. Y. Tang, B. L. Allen, D. R. Kauffman, A. Star, J. Am. Chem. Soc., **2009**, 131, 13200.

173. Z. Chen, D. Higgins, H. Tao, R. S. Hsu, Z. Chen, J. Phys. Chem., **2009**, 113, 21008.

174. S. Kundu, T. C. Nagaiah, W. Xia, Y. Wang, S. Van Dommele, J. H. Bitter, M. Santa, G. Grundmeier, M. Bron, W. M. Schuhmann, J. Phys. Chem., **2009**, 113, 14302.

175. R. Liu, D. Wu, X. Feng, K. Müllen, Angew. Chem., Int. Ed., **2010**, 49, 2565.

176. L. Qu, Y. Liu, J. Baek, L. Dai, ACS Nano, **2010**, 4, 1321.

177. C. Jin, T. C. Nagaiah, WXia, B. Spliethoff, S. Wang, M. Bron, W. Schuhmann, M. Muhler, NanoScale, **2010**, 2, 981.

178. X. Wang, J. S. Lee, Q. Zhu, J. Liu, Y. Wang, S. Dai, Chem. Mater., **2010**, 22, 2178.

179. J. I. Ozaki, S. Tanifuji, A. Furuichi, K. Yabutsuka, Acta, **2010**, 55, 1864.

180. D. B. Williams, C. B. Carter, Transmission electron microscopy a text book for materials science seconnd edition, Springer, New York, USA, **2009**.

181. www.Nobleprize.org/education/Physics/microscopes/TEMindex.htm. 03 July **2011**.

182. V. Mennella, G. Monaco, L. Colangeli, E. Bussoletti, Carbon, **1195**, 33, 115.

183. C. J. Lee, J. Park, J. A. Dean, F. A. Settle, Instrumental method of analysis, sixth edition, New York, USA, **1981**.

184. www.Wikipedia.org/Wiki/thermogravimetric_analysis. 03 July **2011**.

185. H. H. Willard, L. L. Merritt, J. A. Dean, F. A. Settle, Instrumental methods of analysis, Sixth edition, Wadworth publishing company, California, USA, **1981**.

186. www.Wikipedia.org/Wiki/carbon_nanotube. 26 June **2011**.

187. D. B. Warheit, B. R. Lawrence, K. L. Reed, D. H. Roach, G. A. M. Reynolds, T. R. Webb, Toxicol. Sci., **2004**, 77, 117.

188. V. Bajpai, L. Dai, T. Ohashi, J. Am. Chem. Soc. **2004**, 126, 5070.

189. H. Hou, Z. Jun, F. Weller, A. Greiner, Chem. Mater., **2003**, 15, 3170.

# CHAPTER 3

## 3. CVD SYNTHESIS OF NITROGEN DOPED CARBON NANOTUBES USING IRON PENTACARBONYL AS A CATALYST

### 3.1 Introduction

#### 3.1.1 Carbon nanotubes (CNTs)

A carbon nanotube is a hexagonal array of carbon atoms rolled up into a thin, hollow, long cylinder [1]. Carbon nanotubes exist in two forms i) single walled CNTs (SWCNTs) and ii) multi walled CNTs (MWCNTs). SWCNTs have a diameter range from 1 to 10 nm and are normally capped at their ends. In contrast, MWCNTs are larger in diameter and range from 5 nm to a many tens of nanometers. SWCNTs can also form bundles which are held together by van der Waals forces [2,3]. CNTs have remarkable physical and electrical properties, which were discussed in **chapter 2, section 2.2.4.** In addition, CNTs possess high surface areas, high aspect ratios and good mechanical properties [4,5].

Despite their phenomenal properties, the hydrophobicity and chemical inertness of CNTs impede their commercial use. To resolve this problem, scientists have come up with methods to modify the surfaces of CNTs. Their surface properties can then be tailored either by covalent or by non-covalent surface modifications. Covalent modification involves introduction of either new elements (e.g. O, N) onto the CNT or by incorporation of organic functional groups (e.g. bio molecules) onto CNT sidewalls. Noncovalent modification, can be done via adsorption of surfactants, biological macromolecules, and polymers without any intrinsic structural change to the CNTs [6]. Both strategies have been used to fabricate modified CNTs. In the covalent approach, incorporation of the elements, such as fluorine, nitrogen and boron leads to a modification of the CNT density of state which changes their semiconducting properties [7]. In the non-covalent approach, only the CNT surface is

targeted and their surfaces can be modified by addition of polar functional groups that can improve the dispersion and cross linking capabilities of CNTs during polymerization.

In this study the modification of the CNT properties has been achieved by introducing nitrogen atoms into the CNT structure. This process is called doping. The materials once doped are called N-CNTs (nitrogen doped carbon nanotubes). N-CNTs can be prepared by different approaches such as, laser ablation, arc discharge and chemical vapour deposition (CVD). The method which was used in this study was CVD using a floating catalyst method. A floating catalyst method is a common method to fabricate CNTs on a large scale [8,9]. In a floating catalyst method there is no need to utilize a catalyst support, which reduces the cost of CNT production. The type of catalyst required to achieve this method typically is a volatile organometallic complex such as ferrocene (FcH), a substituted FcH (with or without N substituents) or $Fe(CO)_5$ [10]. In this study $Fe(CO)_5$ was used as the floating catalyst. $Fe(CO)_5$ has the advantage than the Fe is in the zero oxidation state and hence, unlike ferrocene and ferrocene derivatives, does not require the presence of a reducing gas such as $H_2$. Further, $Fe(CO)_5$ has been known to be an excellent catalyst for the production of CNTs that are not doped. Indeed the HiPco process is based on the use of $Fe(CO)_5$ in a reactor at high pressure [11].

There are numerous reports on the use of $Fe(CO)_5$ as a catalyst to produce CNTs, but little is known about its ability to produce N-CNTs. An example is a study by Banjapai et.al. [12] who synthesized aligned helical N-CNTs by the co-pyrolysis of $Fe(CO)_5$ and pyridine on a quartz substrate at high temperature (900-1100 $^oC$). A summary of some of the studies that have been reported in the literature is which $Fe(CO)_5$ has been used to make CNTs and N-CNTs is given in **Table 3.1**. As will be seen, $Fe(CO)_5$ has been successfully used to make both SWCNTs and MWCNTs.

**Table 3.1:** Use of $Fe(CO)_5$ as catalyst to make doped and undoped CNTs [13].

| SNCM | Reactor design | Carbon source | Catalyst | Temperature | Pressure and flow rate | References |
|---|---|---|---|---|---|---|
| **SWCNTs** | Horizontal CVD reactor; two stage furnace system | Acetylene | $Fe(CO)_5$ | 350 $^oC$ (furnace 1) 1100 $^oC$ (furnace 2) | $C_2H_2$ flow rate 50 sccm Ar flow rate 1000 sccm ($Fe(CO)_5$ -1 ml) | [14] [15] |
| **SWCNTs** | Horizontal CVD reactor | CO | $Fe(CO)_5$ | 800-1200 $^oC$ | CO (1-10 atm) $Fe(CO)_5$ (1-25 mTorr) | [16] [17] |
| **SWCNTs** | Horizontal CVD reactor; two stage furnace system | CO | $Fe(CO)_5$ | 700 $^oC$ (furnace 1) 900 $^oC$ (furnace 2) | CO flow rate: 800 sccm $H_2$ flow rate: 200sccm | [18] |
| **MWCNTs** | Horizontal CVD reactor; two stage furnace system with vapourization chamber and an ice cooler | 1:1, Pyridine Toluene | $Fe(CO)_5$ | 1050-1150 $^oC$ | $H_2$ flow rate: 350-400 ml/min | [19] |
| **MWCNTs** | Horizontal CVD reactor | pyridine | $Fe(CO)_5$ | 900-1100 $^oC$ | Ar and $H_2$ | [12] |
| **MWCNTs** | Vertical CVD reactor | Methane | $Fe(CO)_5$ | 1050-1150 $^oC$ | $CH_4$ flow rate 125-250 sccm $N_2$ flow rate: 1000-2000 sccm $Fe(CO)_5$ feeding rate 0.5-2.5 mL/h | [20] |

## 3.2 Experimental

### 3.2.1 Chemicals and materials

Toluene and acetonitrile were purchased from Merck, and iron pentacarbnyl was purchased from Fluka. Acetonitrile was distilled before use. All reactions were performed under an Ar atmosphere.

### 3.2.2 Characterization

#### 3.2.2.1 Thermogravimetric analysis

TGA experiments were performed on a Perkin Elmer Pyris 1 TGA analyzer under an air atmosphere in the temperature range 25-900 $^{o}$C at a heating rate of 10 $^{o}$C/min. Peak positions are recorded in units of Celsius.

#### 3.2.2.2 Raman spectroscopy

Raman spectra were acquired using a Jobin-Yvon T64000 Raman spectrograph operated in single spectrograph mode. The excitation source was the 514.5 nm line of an argon ion laser. This was focused onto the sample using a long-working distance 20x objective with an Olympus BX40 microscope attachment. The power at the sample was kept low (< 1.2 mW) to minimise possible localised heating of the sample. The backscattered light was collected using the microscope and dispersed via a 600 lines/mm grating onto a liquid nitrogen cooled CCD detector. The data was acquired using Labspec v4.18 software. Accumulation times varied between 2 and 3 minutes, and the confocal pinhole was set to either 2 mm or 0.5 mm, depending on the degree of background fluorescence.

#### 3.2.2.3 Transmission electron microscopy

TEM studies were performed by using a FEI Technai $G^2$ Spirit electron microscope at 120 kV.

### 3.2.3 Synthetic procedures: Injection method

#### 3.2.3.1 The synthesis of nitrogen doped carbon nanotubes (N-CNTs)

A typical experiment is described below.

Synthesis of N-CNTs was carried out at 900 $^{o}$C under an Ar atmosphere at atmospheric pressure. The flow rate of Ar was kept constant at 300 mL/min. All the precursors were kept under an Ar atmosphere before use. A mixture of toluene (17.5 mL), acetonitrile (3.50 mL) and $Fe(CO)_5$ (1.34 mL) was placed in a 25 mL syringe driven by a SAGE syringe pump. The solution was injected at 0.80 ml/min into a quartz tube reactor (32 cm x 1 m) via a special quartz delivery system cooled by water as shown in **Figure 3.1**. This cooling system allowed the solution to be injected into the hot region of the quartz tube. The reaction took about 20-25 min. After the reaction was done, Ar gas was passed through the tube at approximately 50 mL/min while the reactor cooled to room temperature, carbon soot was removed from the tube, weighed and kept in an air tight vial prior to characterization. **Figure 3.1** shows the reactor which was used.

In related studies the acetonitrile to toluene ratio was varied while the $Fe(CO)_5$ content was maintained at 1.3 mL. In these studies the acetonitrile content ranged from 0% to 25%. A summary of the experimental condition used is shown in **Table 3.2**. Many other variation to the initial reaction were also performed. This included the use of a different temperature (900 $^{o}$C), flow rate (200 mL/min), and a different carrier gas (Ar + 5% $H_2$). All the condition used are shown in **Table 3.2**.

**Table 3.2:** Experimental conditions used for the N-CNTs produced.

| Experiment number | $CH_3CN$ (%) | Temperature ($^oC$) | Gas flow rate (mL/min) | Carrier gas | Yield (g) |
|---|---|---|---|---|---|
| 1 | 0 | 900 | 200 | Ar | 0.65 |
| 2 | 0 | 900 | 300 | Ar | 0.21 |
| 3 | 2 | 850 | 200 | Ar | 0.21 |
| 4 | 2 | 850 | 200 | Ar + 5% $H_2$ | 0.47 |
| 5[a] | 2 | 850 | 300 | Ar | 0.07 |
| 6[a] | 2 | 900 | 200 | Ar | 0.06 |
| 7 | 2 | 900 | 200 | Ar + 5% $H_2$ | 0.27 |
| 8 | 2 | 900 | 300 | Ar | 0.97 |
| 9 | 5 | 850 | 200 | Ar | 0.85 |
| 10 | 5 | 850 | 200 | Ar + 5% $H_2$ | 0.38 |
| 11[a] | 5 | 850 | 300 | Ar | 0.05 |
| 12 | 5 | 900 | 200 | Ar | 0.74 |
| 13 | 5 | 900 | 200 | Ar + 5% $H_2$ | 0.53 |
| 14 | 5 | 900 | 300 | Ar | 0.76 |
| 15 | 15 | 750 | 200 | Ar | 0.05 |
| 16 | 15 | 800 | 200 | Ar | 0.05 |
| 17 | 15 | 850 | 200 | Ar | 0.26 |

| | | | | | |
|---|---|---|---|---|---|
| **18** | **15** | **850** | **200** | **Ar + 5% $H_2$** | **0.38** |
| **19**[a] | **15** | **850** | **300** | **Ar** | **0.03** |
| **20** | **15** | **900** | **200** | **Ar** | **0.66** |
| **21** | **15** | **900** | **200** | **Ar + 5% $H_2$** | **0.58** |
| **22** | **15** | **900** | **250** | **Ar + 5% $H_2$** | **0.26** |
| **23** | **15** | **900** | **300** | **Ar** | **0.40** |
| **24** | **20** | **900** | **200** | **Ar** | **0.78** |
| **25** | **25** | **900** | **200** | **Ar** | **0.71** |

[a] indicates a 10 mL solution.

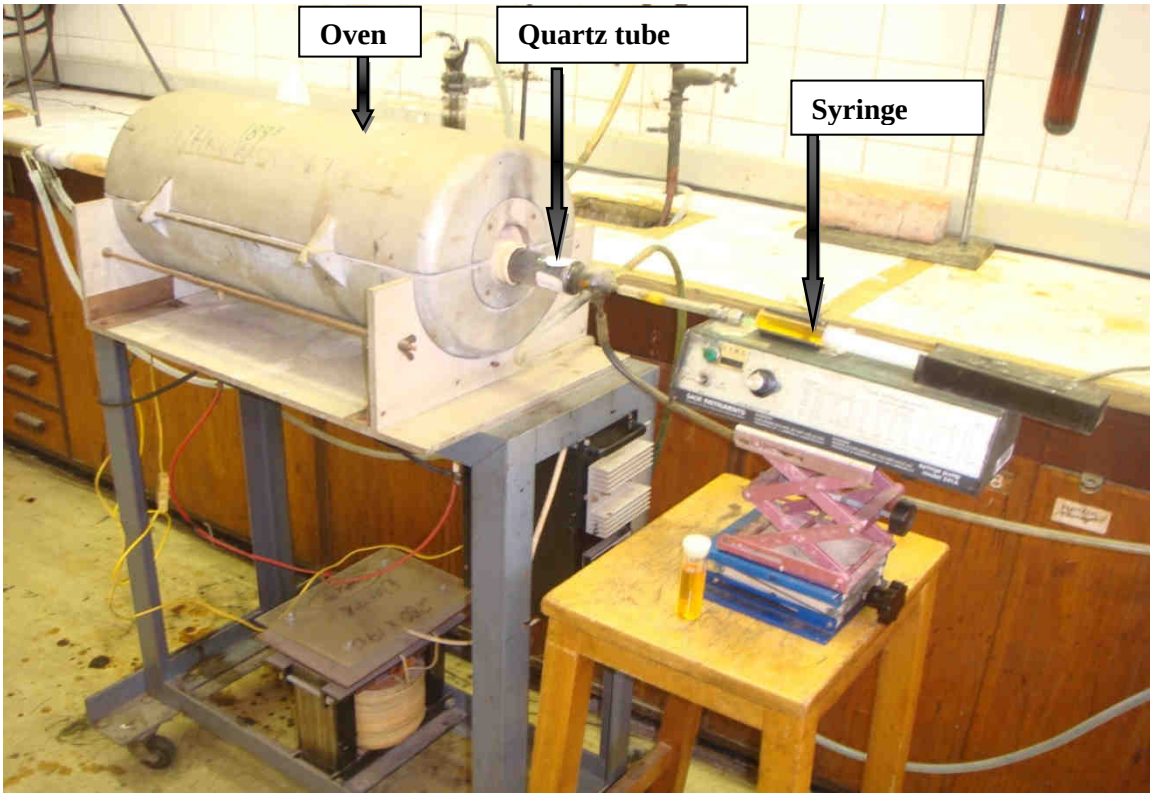


**Figure 3.1 :** A furnace and syringe attachment used for the synthesis the N-CNTS.

#### 3.2.3.2 Purification of N-CNTs

The synthesized N-CNTs were purified by using either $HNO_3$ (55%) or HCl (35%). The purification was carried out at 80 $^oC$ for 6 hours. The solution was cooled to room temperature, filtered and the black powder washed with distilled water several times until the pH of the solution was around 7. The sample was then dried in an oven at 100 $^oC$ overnight.

## 3.3 Results and discussion

### 3.3.1 Synthesis of nitrogen doped carbon nanotubes

Nitrogen doped CNTs with varying degree of abundance and purity were synthesized according to the procedure outlined in the experimental **section 3.2.3.1**. All the samples were washed with acid prior to TGA and Raman analyses. The advantage of using $HNO_3$ rather than HCl is that, $HNO_3$ leads to surface functionalization, specifically at high temperatures. Further, the use of HCl is not desirable when the CNTs are to be used in catalysis applications. It has been reported that the presence of $KMnO_4$ in acidic solution works better and it generates a pure material [21], however this reagent was not used in this study.

TEM studies have shown that the N content affects the tube morphology and bamboo compartment formation. The presence of bamboo compartments is not a sufficient contribution to indicate N incorporation since bamboo-like structures have also been observed in Y-junction CNTs that do not contain N [22]. A TEM study revealed that N incorporation in the CNT structure did form separated compartments. It was reported by Nxumalo et al. [10] that an increase in N % source decreased the compartment distance. This is expected and it agrees with the mechanism proposed for N-CNT growth [23]. N-CNT bamboo compartment separation also increases with an increase in growth temperature [24]. TGA studies confirmed the presence of nitrogen in the CNTs as indicated by the change of decomposition temperatures

observed when the CNTs were removed with $O_2$ in TGA experiments. The more nitrogen incorporated the less stable the N-CNTs that were formed. From a Raman study, an intense D band was observed that indicated the presence of disorder in the tubes. The level of disorder can be determined by measuring the $I_D/I_G$ ratio (see below).

Many variables were changed in the experiments to optimize the growth of the N-CNTs. In the sections below the effect of each of these variables on N-CNT yield, morphology and purity are discussed. In each set of data an attempt has been made to vary only one parameter at a time.

### 3.3.2 Effect of %$CH_3CN$ in toluene

In this study the following conditions were used: reaction temperature-850 $^oC$, gas flow rate-300 mL/min, gas used Ar.

#### 3.3.2.1 Yield study

The effect of the reaction mixture in which the N content was varied by changing the amount of $CH_3CN$ used in a $CH_3CN$/toluene mixture on the yield was studied. It was observed, that an increase in N content, decreased the yield. The $CH_3CN$/toluene ratios used are shown in **Table 3.2** (enteries: 5, 11, 19, entries: 8, 14, 23 and entries: 1, 12, 20). It was also noted that the gas flow rate affected in the yield (**Table 3.2**, entries: 20, 23): the yield decreased with an increase in the gas flow rate.

The effect of nitrogen containing organic compounds on N-CNT growth was reported by Nxumalo et al. [25]. They used different N compounds (e.g. amines, aromatic compounds). It was revealed that after an increase in amine concentration, the yield of CNTs generally decreased. Similar results were found for aromatic reagents (pyridine) and amides.

It is believed that the N concentration plays an important role in terms of yield production. Obviously with an increase in N concentration the yield drops. The reason given is nitrogen slows down the rate of tube growth and when N atoms sit on the surface of the catalyst it retards carbon growth on the catalyst.

### 3.3.2.2 TEM studies

TEM analysis was used to examine the type, quality, size distribution and quantity of N-CNTs produced. TEM analysis allowed a facile measurement of N doping to be determined since doping CNTs with nitrogen leads to the formation of bamboo compartments. An example of a bamboo structure is shown in **Figure 3.2.** The formation of bamboo compartment can be rationalized by its growth mechanism. Generally, what happens is C and N atoms both deposit on the catalyst surface and when they accumulate on the catalyst surface they will both be ejected from the surface and form a separate layer which leads to the bamboo structure as shown in **Figure 3.2**. The formation of the cavities is due to the presence of nitrogen on the catalyst surface.

#### (a) Sample analysis

TEM images were recorded of samples produced (unpurified) from the three different ratios of $CH_3CN$/toluene studied (temperature-850 $^oC$, flow rate-300 mL/min). The images reflect the type of materials produced. The % of each type of sample was determined by considering many tens of such images. A fair estimate of the material could be established. A summary of the data is given in **Table 3.3**.

As is shown in **Table 3.3,** the 5% $CH_3CN$ sample contains the highest amount of tubes compared to the others. Based on the observation from TEM images it is assumed that the shortest tubes were obtained from the 15% sample (**Table 3.2,** entry: 11) and theoretically it can be also confirmed because as the amount of nitrogen increases the length of the tubes decreases due to the presence of the N

atoms. Incorporation of N in the CNT reduces the rate of tube growth and it also terminates the reaction. Similar observations were seen when FcH/aniline was used to make N-CNTs [26]. Generally the lengths shorten with increased N incorporation. The 2% sample (**Table 3.2,** entry: 5) resulted in more straight aligned tubes, whereas the 5% sample (**Table 3.2,** entry: 18) contained bent tubes with a few open tips as shown in **Figure 3.3 e, f**. The details of the TEM images shown in **Figure 3.3** are as follows: a: tubes with a very small amount of amorphous carbon, b: carbon fibers, c: tubes, d: amorphous carbon plus a few tubes, e: tubes, f: tubes with open tips, g: carbon spheres, h: tubes with open tips, i: tubes with bamboo compartments. This variation in morphology is due to the different C:N ratios.

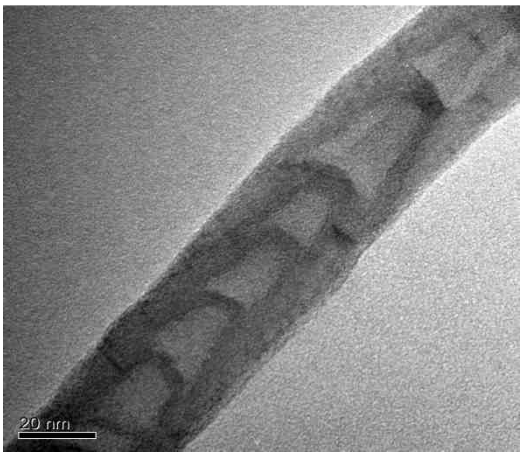


**Figure 3.2:** The TEM image of bamboo structure doped with N.

**Table 3.3**: Samples content as determined by using TEM images.

| **$CH_3CN$ content (%)** | **Spheres (%)** | **Amorphous carbon (%)** | **NCNT/CNT (%)** |
|---|---|---|---|
| **2** | 0 | 60 | 40 |
| **5** | 0 | 20 | 80 |
| **15** | 1 | 29 | 70 |

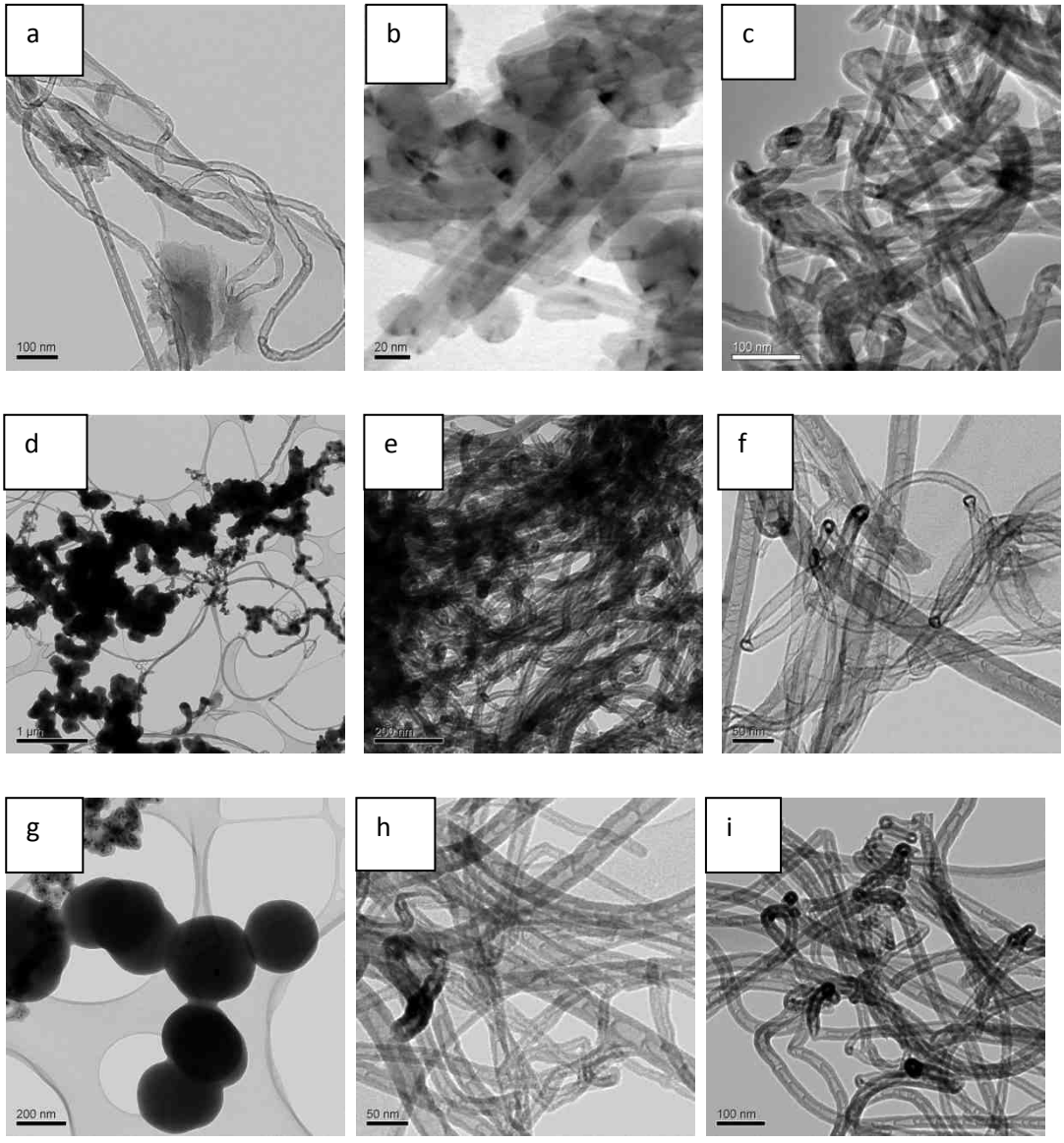


**Figure 3.3:** TEM images of the N-CNT samples produced using $CH_3CN$: 2% (a, b ,c), 5% (d, e, f), 15% (g, h, i) respectively (T: 850 $^oC$, flow rate: 300 mL/min).

**(b) Outer diameter distribution of the N-CNTs**

A focus of this project was on the determination of the yield and morphology of the CNTs. The CNT content (only) of the products produced by varying % $CH_3CN$ used

were studied by TEM. The tubes were viewed by TEM and the outer diameters were measured using the Image J programme. For each sample about 70 tube diameters were measured and these distributions were plotted as shown in **Figure 3.4**. The trends can be seen in **Figure 3.4** and **Table 3.4**.

(a) As the N content increases the tube diameters become smaller. This is in agreement with other literature studies. It has been reported by Nxumalo et al. [25] that the N incorporated in nanotubes made from FcH in benzylamine/toluene had smaller outer diameters but larger inner diameters when compared to undoped CNTs made from FcH/toluene solution under analogous experimental conditions. The same observations were noted when aniline/FcH was used to make N-CNTs [26]. Larger concentrations of the N-source yielded CNTs with smaller diameters. Similar effects were also observed when benzylamine was used as a nitrogen source [27].

(b) At all $CH_3CN$ concentration there is a wide range of outer tube diameters. However, an increase in $CH_3CN$ content gives a narrower distribution of tubes.

**Table 3.4:** The average outer diameter distributions.

| $CH_3CN$% | Avg. outer diameter distributions (nm) |
|---|---|
| 2 | 84 ± 30 |
| 5 | 62 ± 30 |
| 15 | 47 ± 10 |

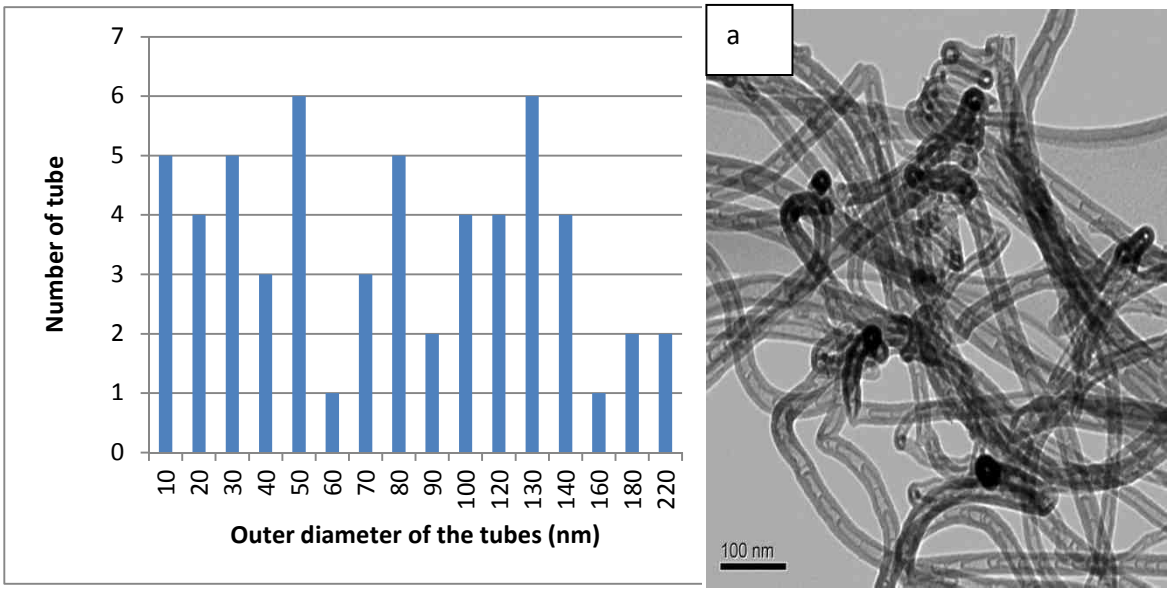
Number of tube
0
1
2
3
4
5
6
7
10
20
30
40
50
60
70
80
90
100
120
130
140
160
180
220
Outer diameter of the tubes (nm)
a
100 nm

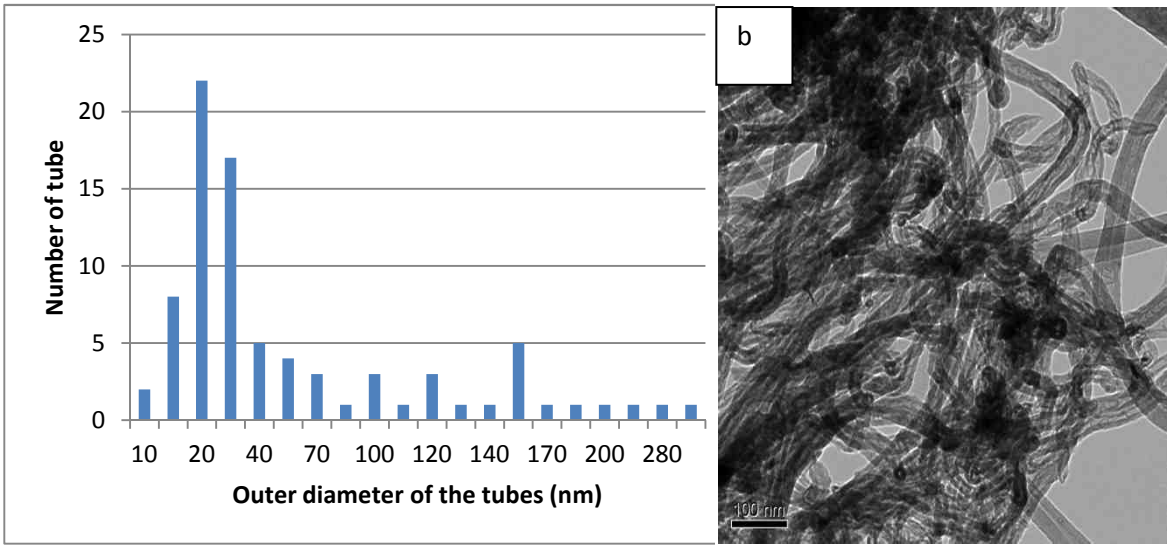
Number of tube
0
5
10
15
20
25
10
20
40
70
100
120
140
170
200
280
Outer diameter of the tubes (nm)
b
100 nm

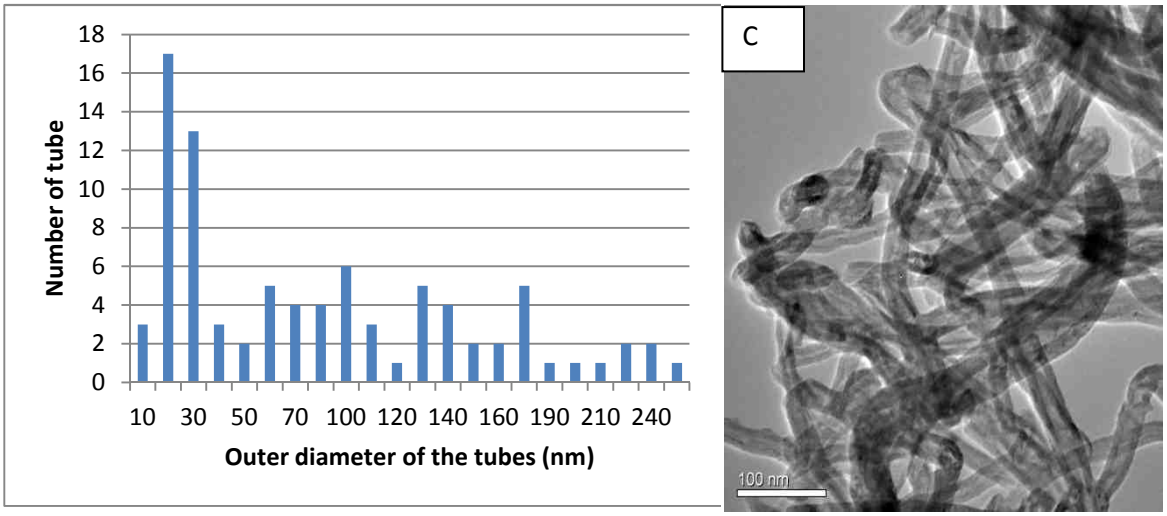


**Figure 3.4:** Graphs of diameter distribution made from 2% (a). 5% (b), 15% (c) of $CH_3CN$, (T: 850 $^oC$, flow rate-300 mL/min).

**(c) Inner diameter distribution of the N-CNTs**

The average inner diameters were measured from TEM micrographs (using Image J) shown in **Table 3.5** As explained, an increase in acetonitrile concentration did not give a change in the inner diameters of the tubes. It was reported by Nxumalo et al. [25], that the N-CNTs made from FcH in benzylamine/touene had smaller outer diameters but larger inner diameters when compared to undoped CNTs grown from a FcH/toluene under the same conditions.

**Table 3.5:** Average inner diameter distribution of the different $CH_3CN$% concentration.

| $CH_3CN$% | Avg. inner diameter distribution (nm) |
|---|---|
| 2 | 26 ± 4 |
| 5 | 29 ± 5 |
| 15 | 20 ± 10 |

**(d) Compartment distance study**

The average distance between bamboo caps was measured from the TEM images (with Image J) shown in **Figure 3.5** for the different samples and average distance are presented in **Table 3.6.** It was revealed that an increase in $CH_3CN$ concentration decreased the compartment distance. This is also shown in **Figure 3.6**. This result is expected and can be explained by the N-CNT growth mechanism which was described in **chapter 2, section 2.2.7.4 (b)** [23]. Similar observations by Nxumalo et al. were also seen [26], when they used different concentration of $PhNH_2$ and $FcPhNH_2$ in their study of N doped CNTs.

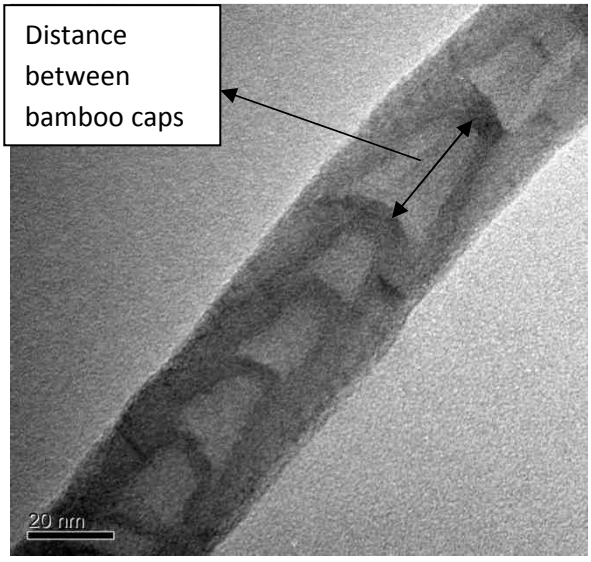


**Figure 3.5:** TEM images of bamboo compartments and the distance between bamboo caps.

**Table 3.6:** Distance between N-CNT bamboo compartments.

| $CH_3CN$% | Avg. distance between individual bamboo compartments (nm) |
|---|---|
| 2 | 28 ± 8 |
| 5 | 22 ± 10 |
| 15 | 9 ± 8 |

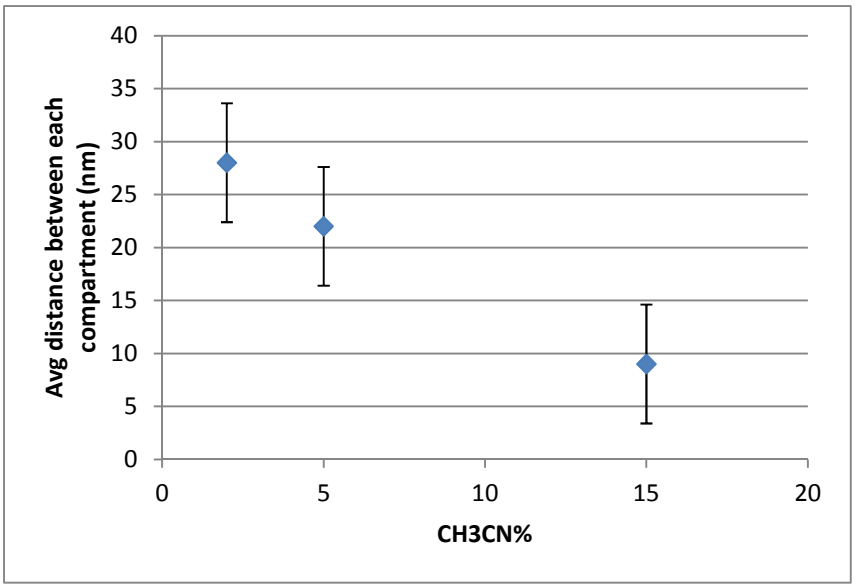


**Figure 3.6:** The average distance between the compartment caps for N-CNTs made from different $CH_3CN$% (T: 900 $^oC$, flow rate: 200 mL/min).

**e) Size of spheres**

The size of spheres were measured using Image J as it shown in **Figure 3.7.** The average size of the spheres was 330 nm for the 15% sample (**Table 3.2,** entry: 19).

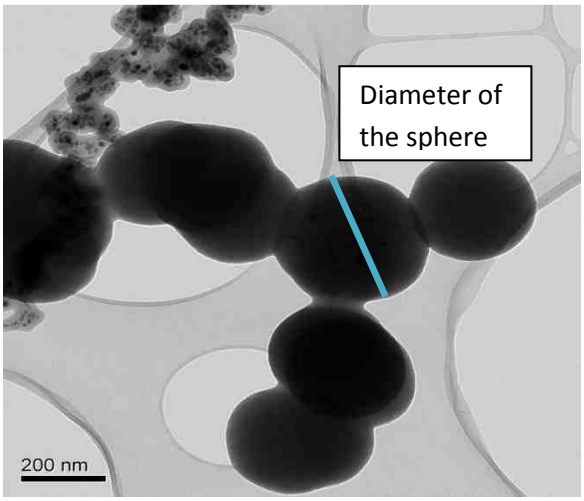


**Figure 3.7:** Synthesized spheres from the 15% sample (T: 850 $^{o}$C, flow rate: 300 mL/min).

### 3.3.2.2 TGA analysis

Thermal stability tests were performed by thermogravimetric analysis. The initial temperature of the oxidative process can be correlated with the presence of lattice defects. The less the defects, the higher the decomposition temperature. The shape of the derivative curve can give some information about the presence of the carbon byproducts. For example, the presence of amorphous carbonaceous particles are burned off first due to the selective etching leading to a faster oxidative etching rate when compared to CNTs. In addition, if a sample contains water or carboxyl groups then a peak around 100 or 300 $^{o}$C would appear respectively. If the rapid oxidation of carbon is fast, the mass loss occurs rapidly giving a smooth curve and it also implies a more perfect crystallinity of the sample. **Figure 3.8** and **Table 3.7** show a comparison of the mass losses of N-CNTs **(A = 0%, B = 5%, C = 15%, D = 25%)** on heating in an air atmosphere at a rate of 10 $^{o}$C min$^{-1}$. In each case the decomposition temperature, determined by measuring the derivatives of the TGA curves, was determined. The example of a derivative curve is shown in **Figure 3.9**.

As the incorporation of N in the CNTs increased the stability of the sample decreased compared to the pristine CNTs. This instability is attributed to the structural disorder introduced by the presence of N into the carbon lattice [28,29]. The TGA data revealed that the N-CNTs thermal stability is less than the undoped one. Similar observation by Nxumalo et al. on the stability of N-CNTs have been reported in the literature [26].

The TGA curves also showed a residual weight (5%). This may relate to the presence of $FeO_x$ residues formed in air from oxidation of the residual catalyst contained in the tubes.

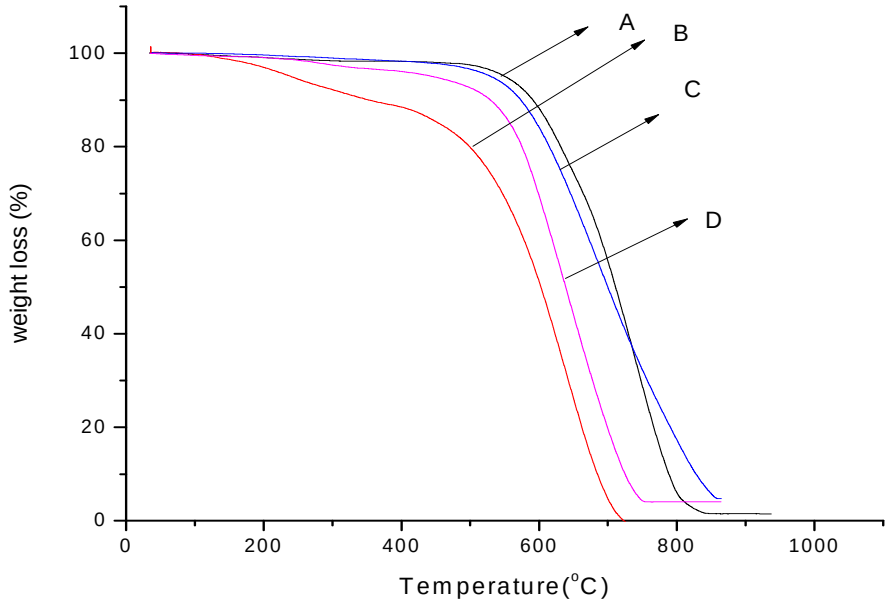


**Figure 3.8**: TGA curves of the purified N-CNTs with different N content (A) 0% , (B) 5%, (C) 15%, (D) 25%.

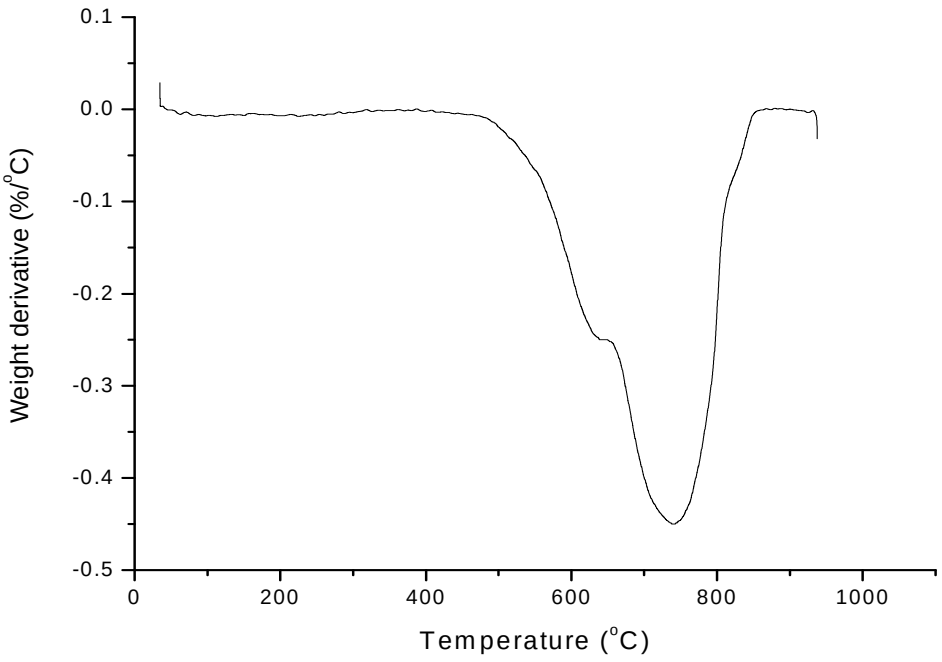


**Figure 3.9:** The derivative curve of 0% $CH_3CN$.

**Table 3.7:** Thermogravimetric analysis of N-CNTs and CNTs **(A-D).**

| **$CH_3CN$%** | **Decomposition temperature $^oC$** |
|---|---|
| **0** | **741** |
| **5** | **641** |
| **15** | **693** |
| **25** | **572** |

### 3.3.2.3 Raman spectroscopy

Raman spectroscopy is an excellent tool to investigate the graphitic structure of carbon materials. Raman spectra generally show two prominent peaks: a G band at approximately 1590 $cm^{-1}$ that corresponds to the Raman active $E_{2g}$ mode and a D band at round about 1390 $cm^{-1}$ that corresponds to disorder features in graphitic sheets. The overall carbon quality can be determined by the $I_D/I_G$ ratio. The higher the $I_D/I_G$ ratio, the lower the graphitic structural quality of the material [26]. It was reported by Koós et al. [30] that the defects increased in the carbon nanotube structure as the amount of benzylamine increased. It was also confirmed in their study, that for $I_D/I_G$ intensity ratios close to one the incorporation of N corresponded to a decreased crystallinty of the CNTs. In a study performed by Nxumalo et al. [26], they observed N-CNTs, produced from ferrocenylaniline/toluene were more disordered than CNTs produced from FcH/toluene alone. It was revealed from Raman analysis that as the concentration of aniline increased in FcH/aniline/toluene mixtures, the degree of disorder also increased. The impact of nitrogen on the structure of CNT reported in the literature suggests that as the concentration of nitrogen increased, the degree of disorder also increased. This implies that N-CNTs produced from 25% $CH_3CN$ should have been more disordered than the CNTs produced from 2% $CH_3CN$. In this study the $I_D/I_G$ ratio difference between the samples with different acetonitrile concentration is very small. **Figure 3.10** and **Table 3.8** and a comparison between Raman spectra for the different $CH_3CN$ concentrations does not give useful information on the topic of disorder**.**

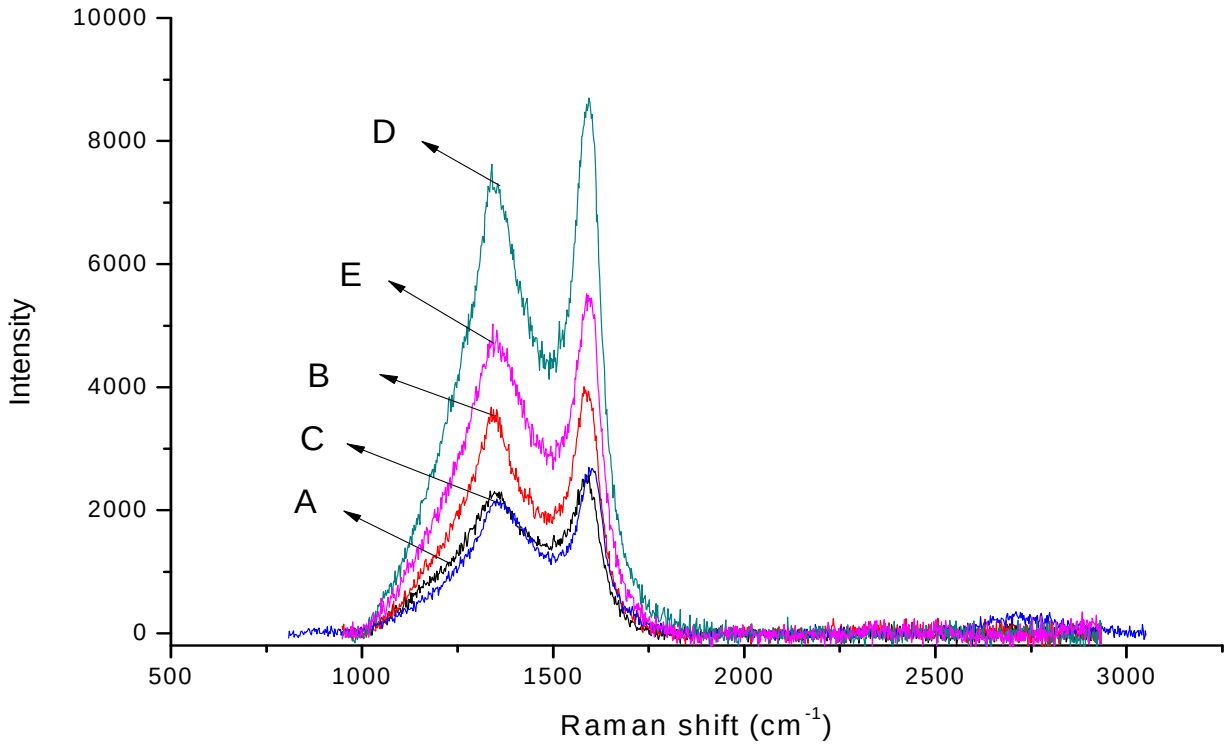


**Figure 3.10:** Raman spectra of the N-CNTs with different N content (A) 2%, (B) 5%, (C) 15%, (D) 20%, (E) 25%.

**Table 3.8:** Raman analysis of the N-CNTs.

| **sample** | **$I_D$** | **$I_G$** | **$I_D/I_G$** |
|---|---|---|---|
| **2%** | **1236** | **1459** | **0.84 ± 0.05** |
| **5%** | **2140** | **2705** | **0.79 ± 0.05** |
| **15%** | **1261** | **1660** | **0.75 ± 0.05** |
| **20%** | **4273** | **5623** | **0.75 ± 0.05** |
| **25%** | **2999** | **3239** | **0.92 ± 0.05** |

### 3.3.3 Effect of temperature

There are a number of experimental parameters that need to be taken into consideration in terms of N-CNT growth. Temperature is a key parameter for the fabrication of N-CNTs. The N-CNT growth temperatures used in this study to make N-CNTs was varied from 750 $^{o}$C to 900 $^{o}$C.

In this study, the effect of four different temperatures were studied. These four reactions were carried out under the same conditions (**Table 3.2** entries: 15, 16, 17, 20). TEM analysis revealed that at 750 and 800 $^{o}$C no tubes were synthesized. At 750 $^{o}$C only fibers (**Figure 3.11 a**) and agglomerates (**Figure 3.11 b**) were observed. At 800 $^{o}$C nanopearl/beads (**Figure 3.11 c**) and nanoparticles embedded into a polymer (**Figure 3.11 d**) were observed. Good quality tubes were observed at both 850 and 900 $^{o}$C **(Figure 3.11 e, 3.11 f, 3.11 g, 3.11 h)**. A sample analysis is displayed in **Table 3.9**. The materials produced when T < 850 $^{o}$C were not studied further.

It has been reported in some papers that N-CNT synthesis is feasible between 700-800 $^{o}$C using other methods or using different catalyst like FcH. Some of these studies are shown in **Table 3.10** [22].

**Table 3.9:** The content of the samples synthesized at different temperature.

| $CH_3CN$ (%) content | Temperature ($^{o}$C) | Spheres (%) | Amorphous carbon (%) | NCNT/CNT (%) |
|---|---|---|---|---|
| 2 | 750 | 0 | 100 | 0 |
| 2 | 800 | 0 | 100 | 0 |
| 2 | 850 | 0 | 20 | 80 |
| 2 | 900 | 0 | 70 | 30 |

**Table 3.10:** Showing the use of different C/N sources and catalyst on fabrication of N-CNTs at different temperatures [22].

| **N/C sources** | **Catalyst** | **T ($^{o}$C)** | **Method** | **references** |
|---|---|---|---|---|
| **4-tert-butylpyridine** | FcH | 700 | CVD | [31] |
| **$NH_3$/pyridine** | FcH | 700-1000 | CVD | [32] |
| **Triphenylphosphine/benzylamine** | FcH | 720 | CVD | [33] |
| **$C_2H_2/NH_3$** | $Fe(CO)_5$ | 750-950 | CVD | [34] |
| **Pyridine, pyrimidine** | FcH | 750 | CVD | [35] |
| **Ethylenediamine** | Co, FcH | 780 | CVD | [36] |
| **Ethanol/benzylamine** | FcH | 800 | CVD | [37] |

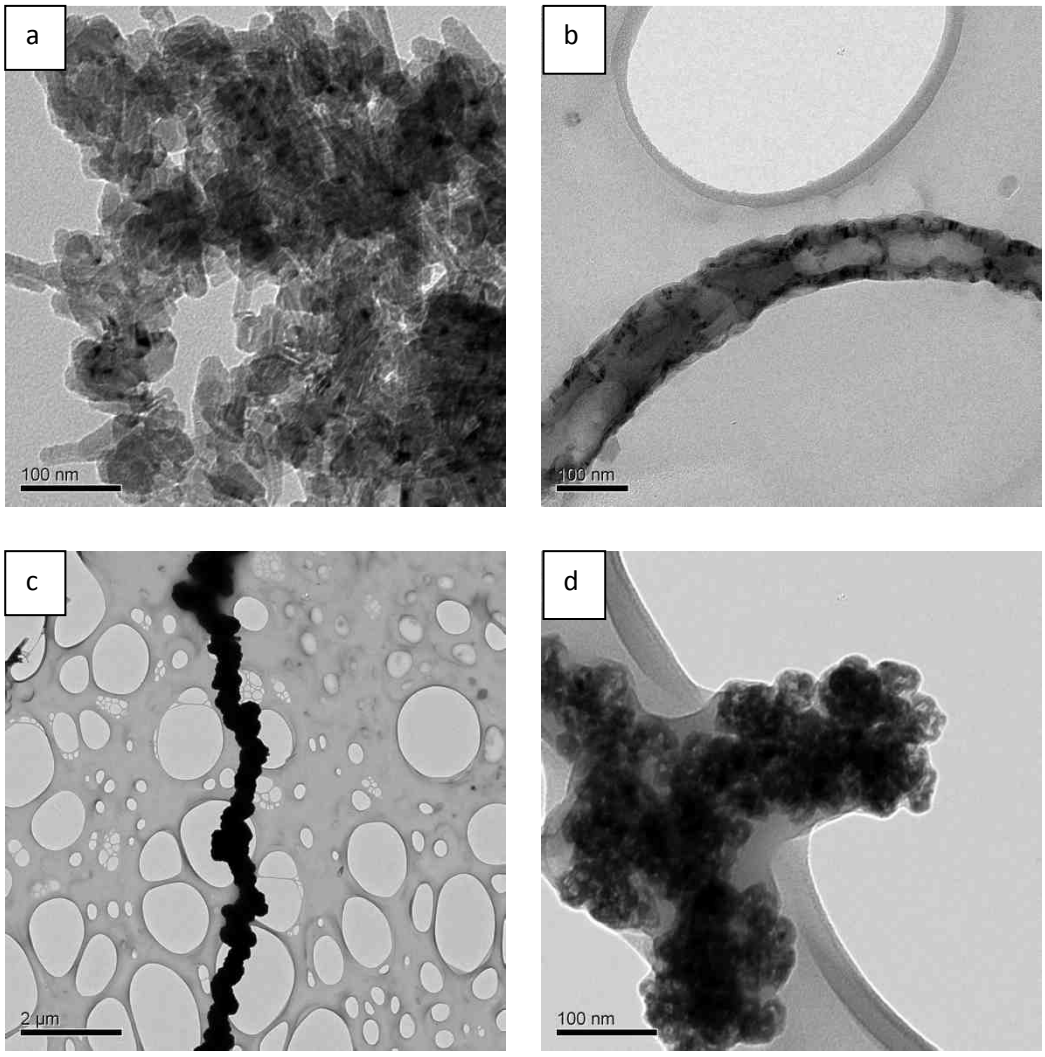
a
100 nm
b
100 nm
c
2 µm
d
100 nm

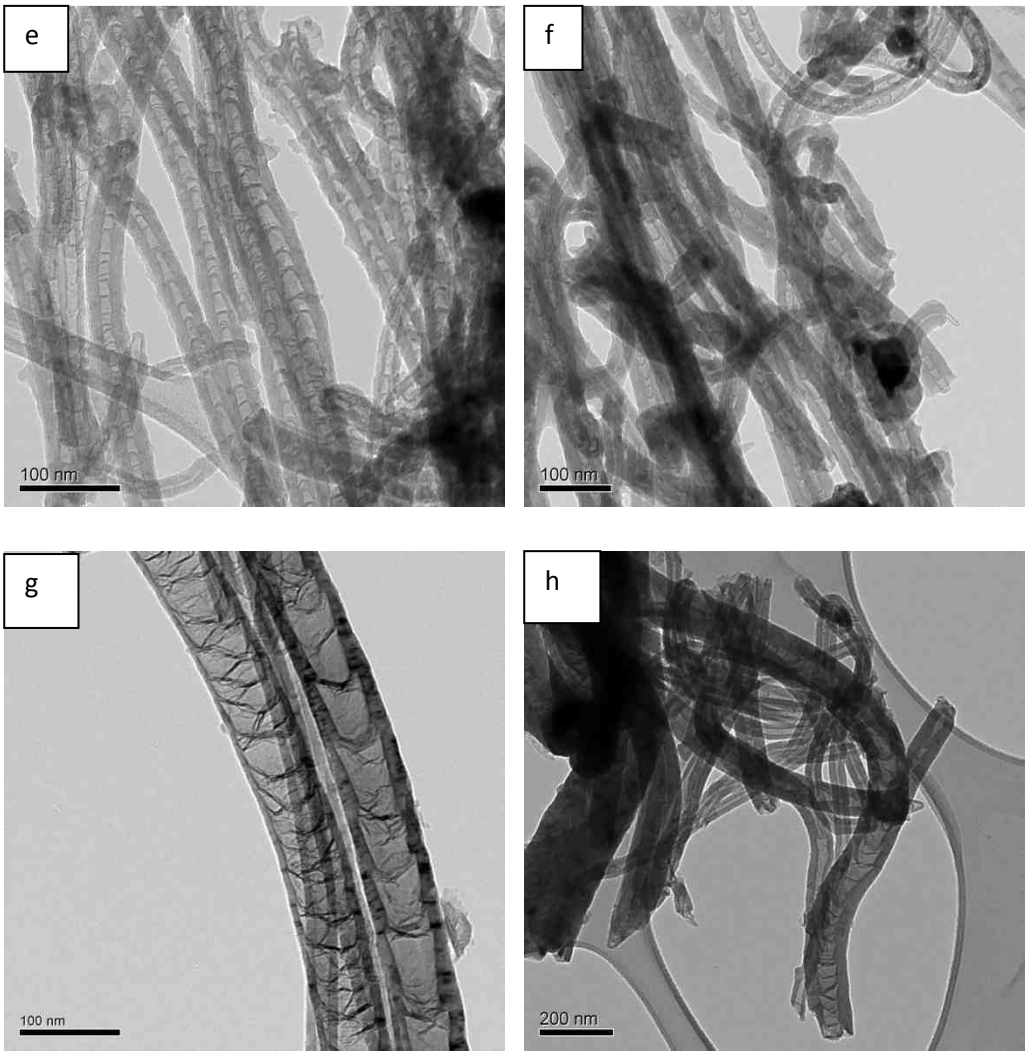


**Figure 3.11:** TEM images of the samples synthesized at 750 $^{o}$C (a-b), 800 $^{o}$C (c-d), 850 $^{o}$C (e-f), 900 $^{o}$C (g-h) (% $CH_3CN$: 15% flow rate: 200 mL/min).

**i) Effect of temperature on the outer diameter distribution**

The study of outer diameter distribution at different temperatures revealed that at both temperatures there is a wide range of tube outer diameters **Figure. 3.12**. It is noticeable that material synthesized at 850 $^{o}$C (graph a) shows a better trend of outer diameter distribution and contained narrower tubes compared to tubes made at 900 $^{o}$C (graph b).

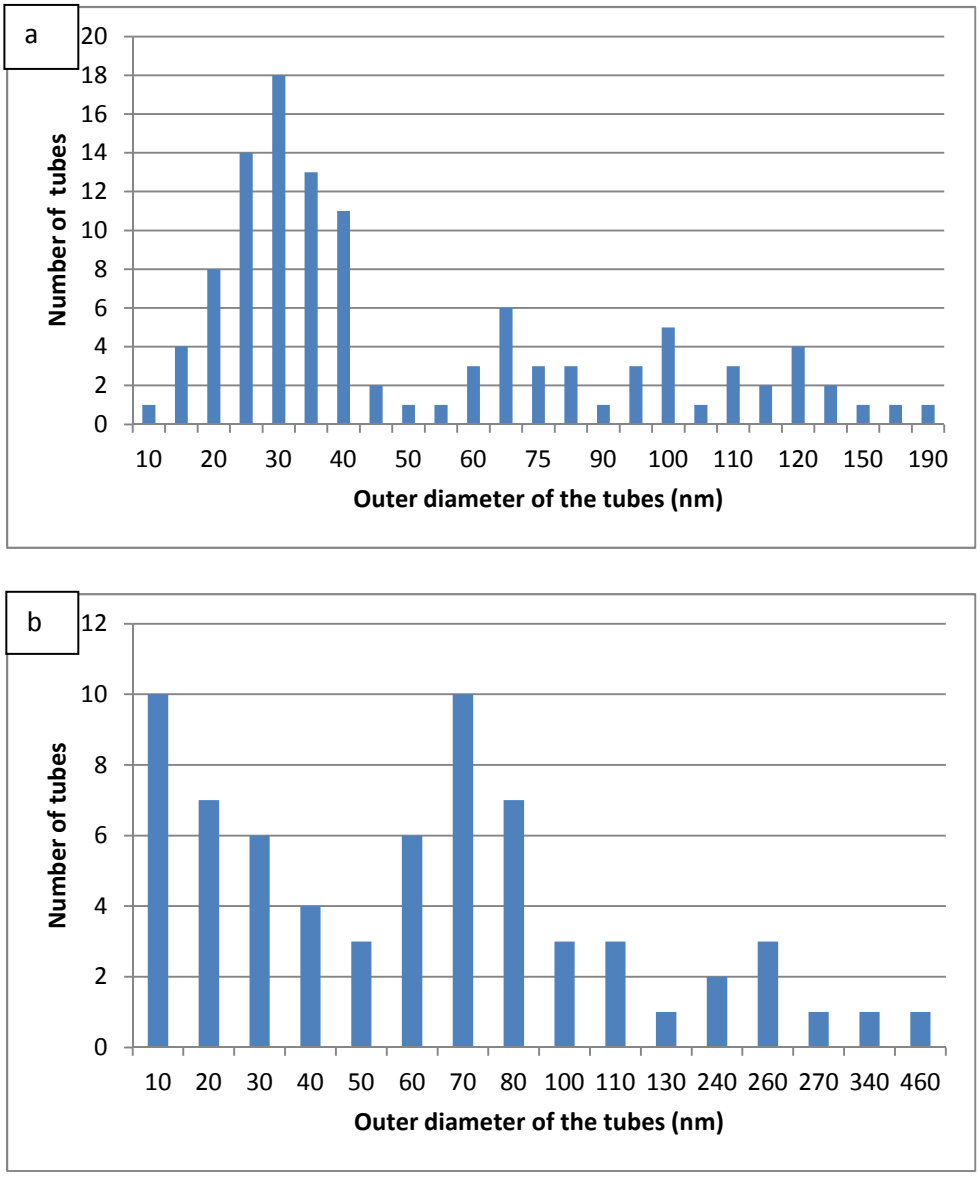


**Figure 3.12:** Graph of diameter distribution of N-CNTs synthesised at a) 850 $^{o}$C, b) 900 $^{o}$C.

### ii) Effect of temperature on the bamboo compartments

From TEM images the average distance between the bamboo caps was measured (100 compartments per sample) using Image J. It was revealed that no major

difference can be seen as a function of temperature at 850 $^{o}$C and 900 $^{o}$C in **Table 3.11.** Note: no tubes were synthesized at 800 $^{o}$C.

**Table 3.11:** The avgerage distance between individual bamboo compartment at 850 and 900 $^{o}$C.

| **$CH_3CN$%** | **Temperature $^{o}$C** | **Avg. distance between individual bamboo compartment (nm)** |
|---|---|---|
| **15** | **850** | **6** |
| **15** | **900** | **5** |

### 3.3.4 Effect of carrier gas

Some experiments were performed in order to evaluate the role of the carrier gas type (Ar or Ar + 5% $H_2$) on the product formation. In this instance $H_2$ was added to the Ar carrier gas to evaluate the effect of $H_2$ on the CNTs produced. The presence of $H_2$ should in principle not play an important role when $Fe(CO)_5$ is used. $H_2$ is a reducing agent and is used to keep the metal in its lowest oxidation state. For example in terms of using FcH hydrogen reduces $Fe^{+2} \longrightarrow Fe^{0}$ but $Fe(CO)_5$ contains Fe in the zero oxidation state so there is no need for a reducing agent.

**i) The effect of hydrogen on carbon yield**

The effect of $H_2$ on the reaction was to give a higher yield of product (**Table: 3.12**). More importantly the addition of $H_2$ also resulted in a change in the morphology of the products produced. As can be seen in **Table 3.12** a higher yield of CNTs were produced.

**Table 3.12:** The experimental conditions used for N-CNT production.

| sample | Carrier gas | Flow rate (mL/min) | Temperature ($^{o}$C) | Yield (g) |
|---|---|---|---|---|
| **15%** | **Ar** | **200** | **850** | **0.26** |
| **15%** | **Ar + 5% $H_2$** | **200** | **850** | **0.38** |

**ii) The effect of hydrogen on type of carbon production**

As mentioned, it was thought that hydrogen would not play an important role in N-CNT production. However the presence of $H_2$ influenced the yield and also the quality of the carbon produced. In this case it reduced the amount of amorphous carbon as shown in **Table 3.13.** Wasal et al. have carried out a study on the CVD synthesis of MWCNTs and they investigated the role of hydrogen on CNT synthesis utilizing FcH as catalyst and xylene as the carbon source [38]. The study revealed that hydrogen caused a competition between the formation of different compounds (soot, carbon fibers and CNTs) and it also reduced the rate of carbon production by dehydrogenation. Consequently more ordered and more thermodynamically stable MWCNTs were produced. Presumably the same effect is observed here.

**Table 3.13:** Shows the effect of hydrogen on the quality of sample content.

| **Sample** | **Carrier gas** | **Sphere (%)** | **Amorphous (%)** | **N-CNTs (%)** |
|---|---|---|---|---|
| **15%** | **Ar** | **0** | **20** | **80** |
| **15%** | **Ar + $H_2$** | **0** | **10** | **90** |

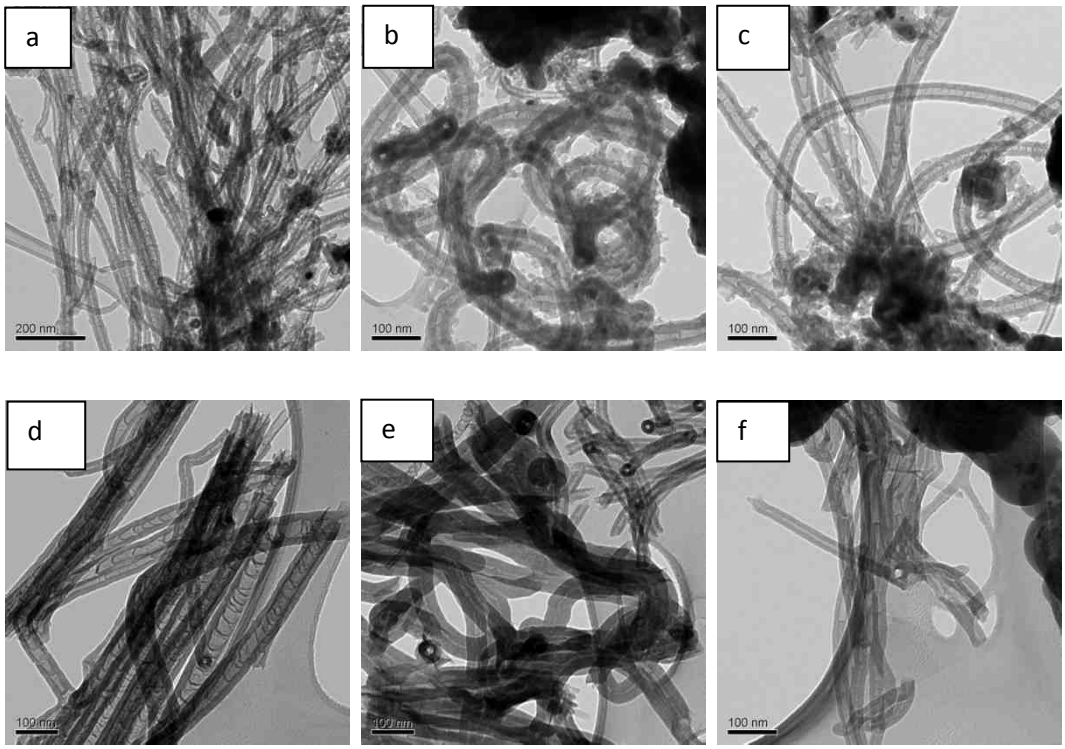


**Figure 3.13:** TEM images of N-CNTs produced using different carrier gases: Ar (a, b, c), Ar + 5% $H_2$ (d, e, f) (15% $CH_3CN$ in toluene, T: 850 $^oC$, flow rate: 200 mL/min).

### iii) The effect of hydrogen on the CNT outer diameters

This analysis revealed that Ar gas without hydrogen produced tubes with a narrower range of diameters as shown in **Figure 3.14**. This figure also indicates that most of the tubes have a diameter of 25 nm when no $H_2$ is present whereas in the second graph (b) ($H_2$ now added to Ar) most tubes have a larger diameter and show a broader range of diameters.

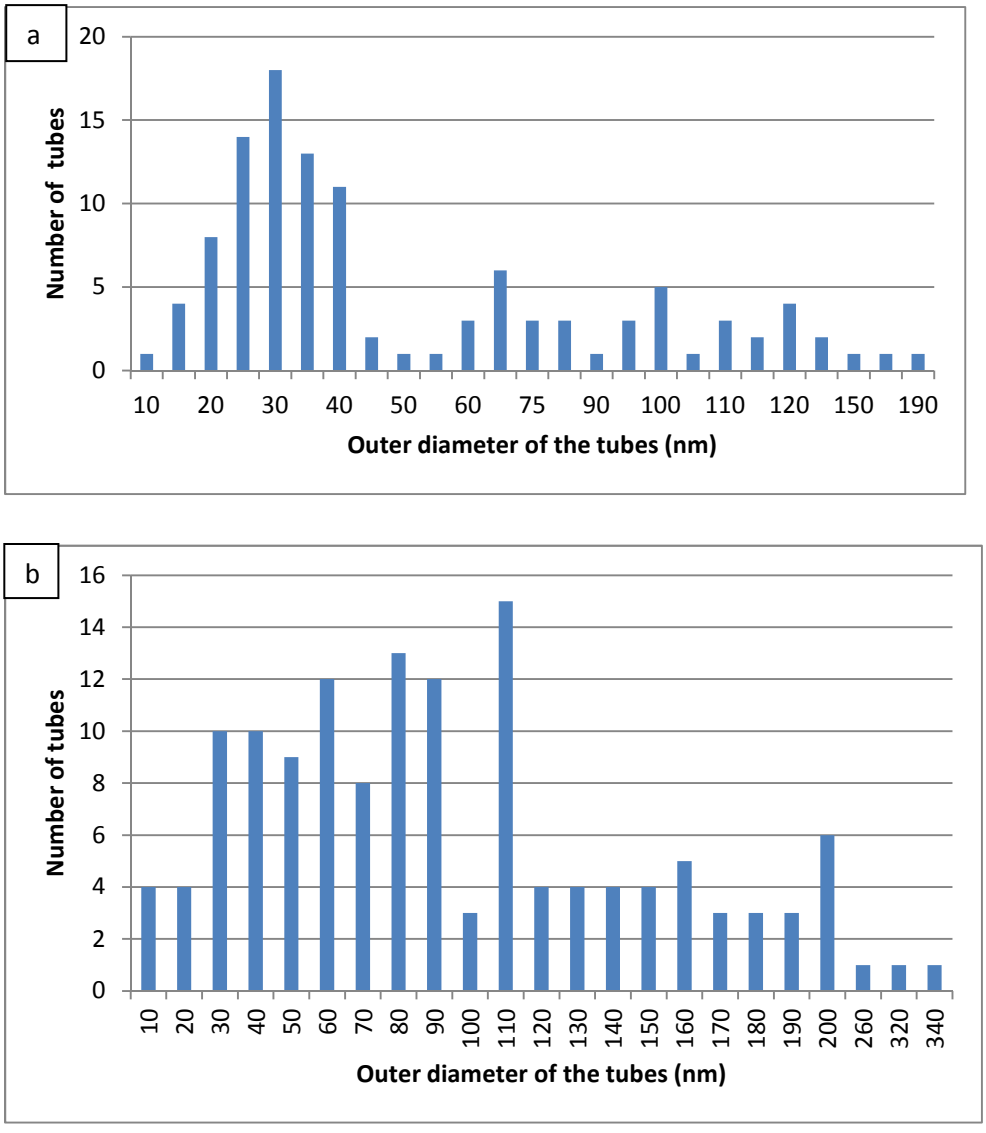


**Figure 3.14:** Graphs of diameter distributions using different carrier gas a) Ar, b) Ar + 5% $H_2$ (15% $CH_3CN$ in toluene, T: 850 $^oC$, flow rate 200 mL/min).

### 3.2.4 Synthesis procedure: Bubbling method

#### i) Synthesis of N-CNTs

A bubbling method was also used to produce N-CNTs. **Table 3.14** show the reaction conditions used for production of the N-CNTs using the bubbling method**.** In this study only one parameter was changed at a time and the ratio of $Fe(CO)_5$/acetonitrile was kept constant at 90%.

**Table 3.14:** The experimental conditions used for the synthesis of N-CNTs.

| Sample number | $CH_3CN$ (mL) | $Fe(CO)_5$ (mL) | Temperature ($^oC$) | Gas flow rate (mL/min) | Carrier gas | solution temperature ($^oC$) | Reaction time (min) | Yield (g) |
|---|---|---|---|---|---|---|---|---|
| 1 | 5.1 | 0.67 | 800 | 200 | Ar | RT | 60 | 0.03 |
| 2 | 5.1 | 0.67 | 800 | 300 | Ar | 75 | 30 | 0.01 |
| 3 | 5.1 | 0.67 | 850 | 200 | Ar | 40 | 30 | 0.01 |
| 4 | 10.2 | 1.34 | 850 | 300 | Ar | RT | 60 | 0.08 |
| 5 | 10.2 | 1.34 | 900 | 300 | Ar | RT | 30 | 0.06 |
| 6 | 10.2 | 1.34 | 900 | 300 | Ar | RT | 60 | 0.06 |
| 7 | 10.2 | 1.34 | 900 | 100 | Ar | RT | 30 | 0.03 |

#### ii) Results and discussion

One of the more common problems which occurs in the injection method is blockage of the injector. This is due to decomposition of the $Fe(CO)_5$ in the tip of the syringe.

To overcome this problem a bubbling method was used to generate N-CNTs. In this method argon was bubbled through a solution of $Fe(CO)_5$ and acetonitrile. The $Fe(CO)_5$ and the acetonitrile will have different vapour pressures and hence their volatility of the two ligands will be different. Thus, in these experiments control in terms of N-CNT formation is more difficult. Notwithstanding this issue, a study was undertaken to evaluate the effect of certain variables (flow rate, temperature, reagent ratios) on the products formed. It was observed that $CH_3CN$ and $Fe(CO)_5$ mixed well together in the absence of the solvent (toluene). The bubbling method resulted in the production of a very good quality of N-CNTs with only a very small amount of amorphous carbon produced. However the bubbling method gave a poor yield of products, even after 30 min bubbling time at room temperature (2 mL out of the 10 mL solution was evaporated). To increase the yield the solution was heated up to 40-75 $^oC$ (below the b.p of $Fe(CO)_5$ (**Table 3.14**, entries: 2, 3), This did not resolve the yield problem. The time of reaction was increased from 30 min to 60 min but again no significant change in yield was observed.

**iii) Yield study**

The effect of different conditions on the product yield was studied and it was observed that the highest yield produced was 0.08 g under the conditions: temperature: 850 $^oC$, gas flow rate: 300 mL/min at a reaction time of 60 min. The lowest yield obtained under the different conditions occurred: when using the condition of temperature-800 $^oC$; gas flow rate-300 mL/min bubbled at 75 $^oC$ and at temperature-850 $^oC$; gas flow rate-200 mL/min bubbled at 40 $^oC$.

It also noticed from the comparison between these experiments (**Table 3.14** entries: 5 and 7), that when the flow rate decreased (from 300 mL/min to 100 mL/min) the yield also decreased. The effect of temperature on the yeild can also be seen in **Table 3.14** (entries: 4 and 6). As the temperature increased the yeild decreased although the change was minor.

**iv) TEM studies**

TEM was the only characterization technique which was used to study the products of these reactions. Based on TEM images it is clear that the bubbling method produced better quantity N-CNTs. The method produced N-CNTs with more corrugated compartments than bamboo like structures. The TEM images revealed that the N-CNTs produced from the solution heated to 40 $^{o}$C contained the highest number of tubes **Figure 3.15 e, f,** whereas when the solution was heated to 75 $^{o}$C tubes with lots of amorphous materials were observed **Figure 3.15 c, d**. When the gas flow rate dropped to 100 mL/min very few tubes were formed **Figure 3.15 m, n**.

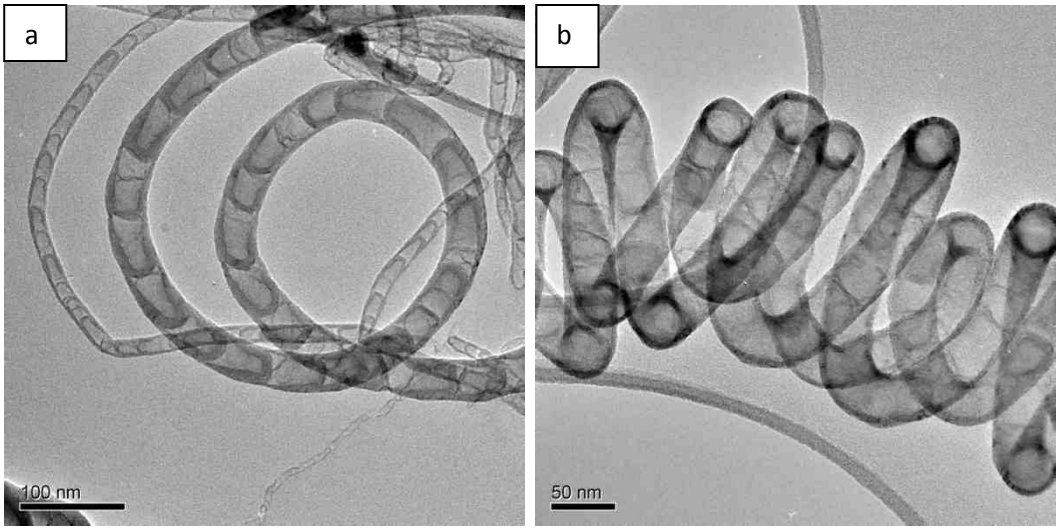

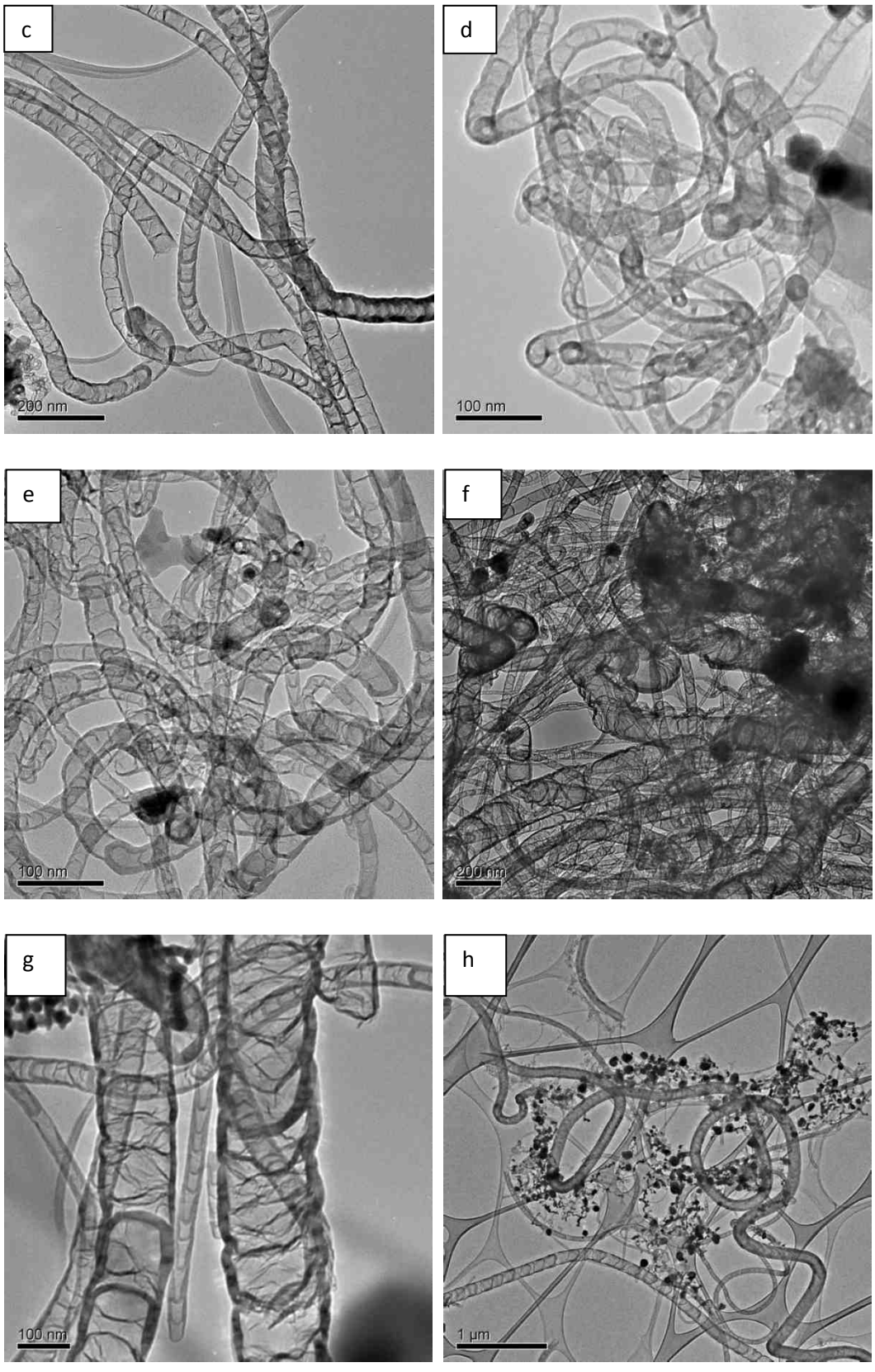
c
200 nm
d
100 nm
e
100 nm
f
200 nm
g
100 nm
h
1 µm

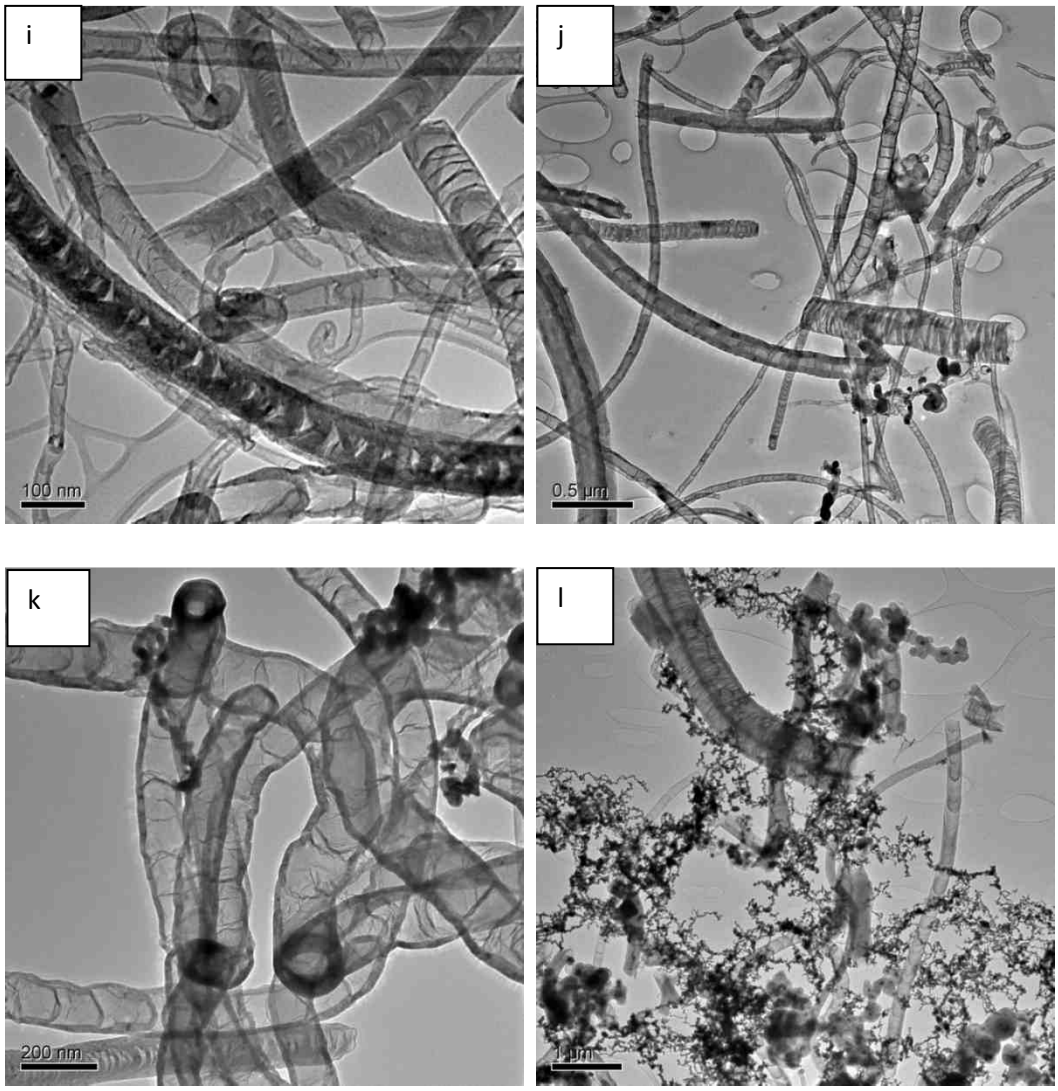
i
100 nm
j
0.5 µm
k
200 nm
l
1 µm

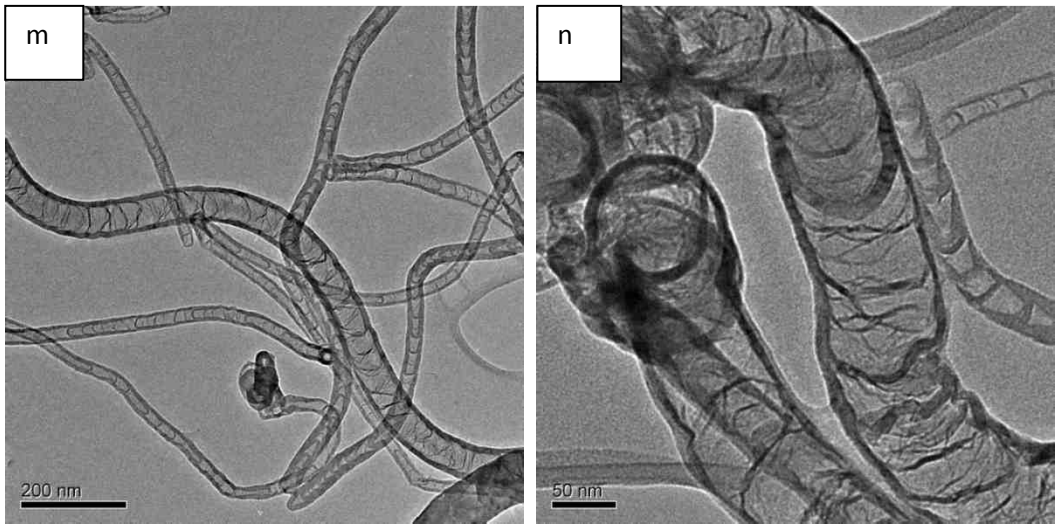


**Figure 3.15:** TEM images of the N-CNTs produced under different conditions. Figures a, b (T: 800 $^{o}$C, flow rate: 200 mL/min, bubbled at RT), c, d (T: 800 $^{o}$C, flow rate: 300 mL/min, bubbled at 75 $^{o}$C), e, f (T: 850 $^{o}$C, flow rate: 200 mL/min, bubbled at 40 $^{o}$C), g, h (T: 850 $^{o}$C, flow rate: 300 mL/min, bubbled at RT), i, j (T: 900 $^{o}$C, flow rate: 300 mL/min, bubbled at RT), k, l (T: 900 $^{o}$C, flow rate: 300 mL/min, bubbled at RT), m, n (T: 900 $^{o}$C, flow rate: 100 mL/min, bubbled at RT).

**v) Outer diameter distribution**

The samples were viewed by TEM and the outer diameters were measured using Image J as shown in **Figure 3.16.** The average of the outer diameter was measured and given in **Table: 3.15.** It is noticed that the samples recorded in graphs a and d (**Table 3.14, entries: 1, 6**) show narrower tubes when compared to samples recorded as entries: 2, 3.

**Table 3.15:** Displays the average outer diameter under different conditions.

| Sample number | Avg diameter (nm) |
|---|---|
| **1** | **49 ± 20** |
| **6** | **46 ± 20** |
| **2** | **58 ± 10** |
| **3** | **74 ± 10** |

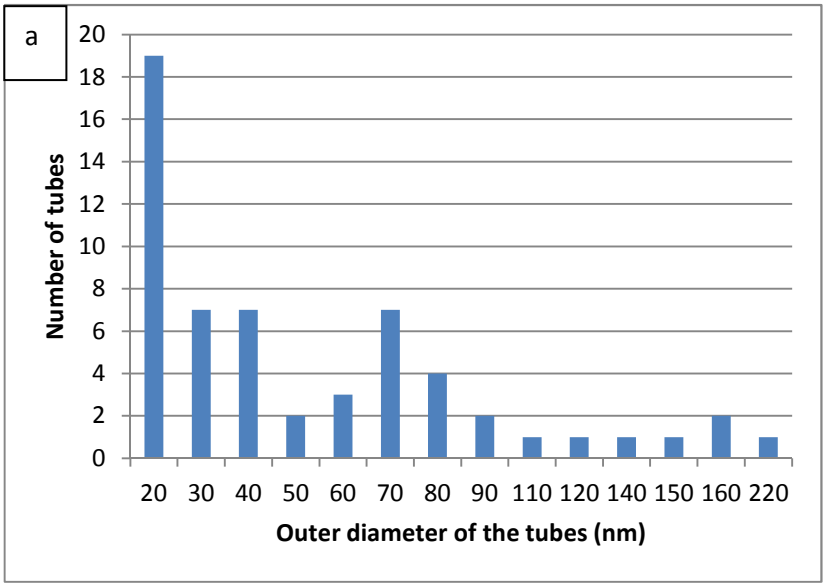

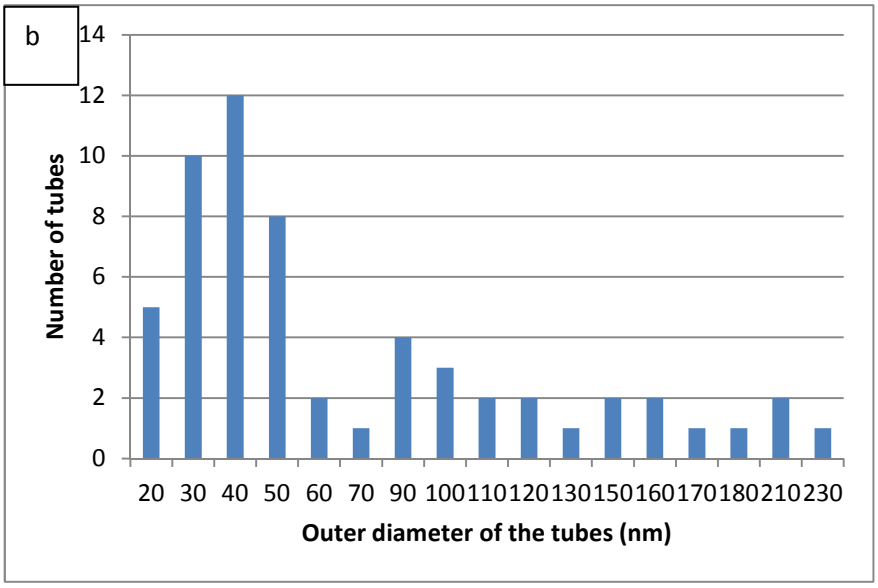
b
14
12
10
8
6
4
2
0
Number of tubes
20 30 40 50 60 70 90 100 110 120 130 150 160 170 180 210 230
Outer diameter of the tubes (nm)

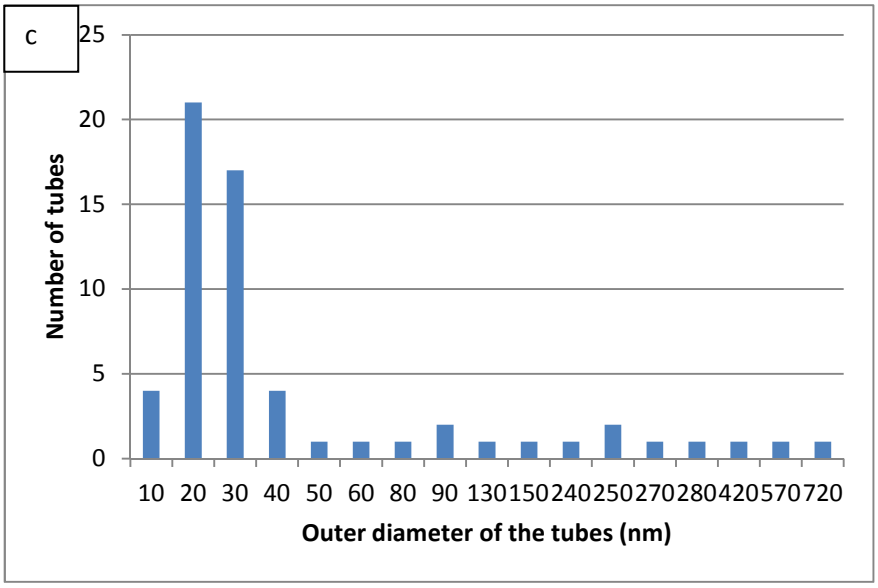
c
25
20
15
10
5
0
Number of tubes
10 20 30 40 50 60 80 90 130 150 240 250 270 280 420 570 720
Outer diameter of the tubes (nm)

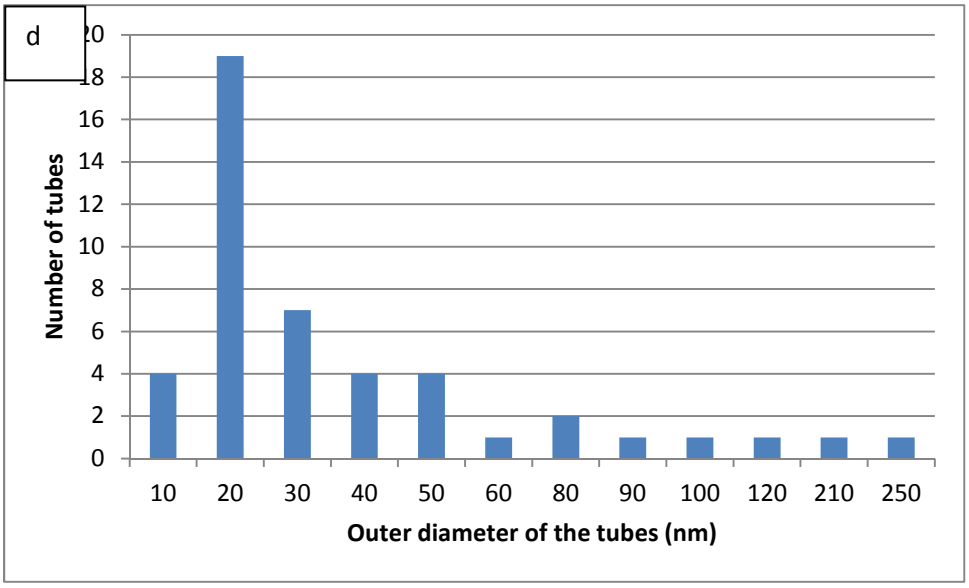


**Figure 3.16:** Graphs of diameter distributions for the N-CNTs produced under different conditions, a ( T: 800 $^{o}$C, flow rate: 200 mL/min), b (T: 800 $^{o}$C, flow rate: 300 mL/min, bubbled at 75 $^{o}$C), c (T: 850 $^{o}$C, flow rate: 200 mL/min bubbled at 40 $^{o}$C), d (T: 900 $^{o}$C, flow rate: 300 mL/min).

### 3.4 Conclusion

The study using $Fe(CO)_5$ as catalyst to make N-doped CNTs has shown that this can be achieved. In this study variables such as methods to produce N-CNTs, $Fe(CO)_5$/acetonitrile ratios, flow rates, temperatures and the addition of $H_2$ to the Ar carrir gas were studied.

Our results showed that: the bubbling method resulted in the production of a very good quality of N-CNTs with formation of a very small amount of carbon byproducts. However, the injection method gave a higher yield of products compared to the bubbling method. The injection method also required less reaction time than the bubbling method to produce more material. The variation of $Fe(CO)_5$/acetonitrile ratios indicated that an increase in acetonitrile concentration led to formation of more tubes with bamboo structures with narrower outer diameters. It was revealed by TGA

that an increase in N concentration decreased the thermal stability of the samples compared to the undoped CNTs. This instability is atributted to the structural disorder introduced by the presence of nitrogen. The impact of temperature on the tube outer diameter revealed that at 850 $^{o}$C a better trend of outer diameter with narrower tubes was achieved compared to tubes produced at 900 $^{o}$C. When $H_2$ added to the Ar it improved the yield and the formation of more tubes with small amount of amourphous carbon. In conclusion, the study showed that $Fe(CO)_5$ can be used as a catalyst in the presence of acetonitrile as a nitrogen source to produce N-CNTs.

### 3.5 References


1. T. Masciangioli, W. X. Zhang, Environ. Sci., **2003**, 37, 102.

2. X. Kitipornchai, K. M. Leiw, J. Solid. Struct., **2005**, 42, 6032.

3. M. Terrones, W. K. Hsu, H. W. Kroto, D. R. M. Walton, A revolution in materials science and electronics, Springer, Berlin, Germany, **1999**.

4. T. W. Ebbesen, H. J. Lezec, H. Hiura, J. W. Bennett, H. F. Ghaemi, T. Thio, Nature, **1996**, 381, 678.

5. J. M. Gibson, T. W.Ebbensen, M. M. J. Treacy, Nature, **1996**, 381, 678.

6. J. Cheng, K. A. S. Fermando, L. M. Veca, Y. P. Sun, A. I. Lamond, Y. W. Lam, S. H. Cheng, ACS. Nano., **2008**, 2, 2085.

7. B. Chandra, J. Bhattacharjee M. Purewal, Y. W. Son , Y. Wu, M. Huang, H. Yan, T.F. Heinz, P. Kim, J. B. Neaton , J. Hone, Nano Lett., **2009**, 9, 1544.

8. P. Nikolaev, J. Bronikowski, R. K. Bradley, F. Rohmund, D. T. Colbert, K. A. Smith, R. E. Smalley, Chem. Phys. Lett., **1999**, 313, 91.

9. O. A. Nerushev, M. Sveningsson, L. K. L. Falk, F. J. Rohmund, J. Mat. Chem., **2001**, 11, 1122.

10. E. N. Nxumalo N. J. Coville, Materials, **2010**, 21, 2141

11. M. J. Bronikowski, P. A. Willis, D.T.Colbert, K. A. Smith, R. E. Smalley. J. Vac. Sci. Tech., **2001**, 19, 1800.

12. V. Bajpai, L. Dai, T. Ohashi, J. Am. Chem. Soc., **2004**, 126, 5070.

13. V. O. Nyamori, S. D. Mhlanga, N. J. Coville, J. Organomet. Chem., **2008**, 693, 2205.

14. B. C. Satishkumar, A. Govindaraj, R. Sen, C. N. R. Rao, Chem. Phys. Lett., **1998**, 293, 47.

15. C. N. R. Rao, A. Govindaraj, Acc. Chem. Res., **2002**, 35, 998.

16. P. Nikolaev, M. J. Bronikowski, R. K. Bradley, F. Rohmund, D. T. Colbert, K. A.

Smith, R. E. Smalley, Chem. Phys. Lett., **1999**, 313, 91.

17. M. J. Bronikowski, P. A. Willis, D. T. Colbert, K. A. Smith, R. E. Smalley, J. Vac. Sci. Tech., **2001**, 19, 1800.

18. S. Huang, X. Cai, C. Du, J. Liu, J. Phys. Chem., **2003**, 107, 13251.

19. H. Hou, Z. Jun, F. Weller, A. Greiner, Chem. Mater., **2003**, 15, 3170.

20. C. S. Kuo, A. Bai, C. M. Huang, Y. Y. Li, C. C. Hu, C. C. Chen, Carbon, **2005**, 43, 2760.

21. K. Herandi, A. Siska, L. Thien-Nga, L. Forro, I. Kiricsi, Solid State Ionic, **2001**, 141, 203.

22. R. M. Yadav, D. P. Singh, T. Shripathi, O. N. Srivastava, J. Nanopart. Res., **2008**, 10, 1349.

23. J. Feng, Y. Li, F. Hou, X. Zhong, Mater. Sci. Eng., **2008**, 473, 238.

24. J. W. Jang, C. E. Lee, S. C. Lyu, T. J. Lee, C. J. Lee, Appl. Phys. Lett., **2004**, 84, 2877.

25. E. N. Nxumalo, P. J. Letsoalo, L. M. Cele, N. J. Coville, J. Organomet. Chem., **2010**, 695, 2596.

26. E. N. Nxumalo, V. O. Nyamori, N. J. Coville, J. Organomet. Chem., **2008**, 693, 2942.

27. X.Y. Tao, X.B. Zhang, F.Y. Sun, J.P. Cheng, F. Liu, Z.Q. Luo, Diamond Relat. Mater., **2004**, 16, 425.

28. R. Kurt, A. Karimi, Chem. Phys. Chem., **2001**, 2, 388.

29. X. Ma, E. G. Wang, Appl. Phys. Lett., **2001**, 78, 978.

30. A. A. Koós, F. Dillon, E. A. Obraztsova, A. Crossley, N. Grobert, Carbon, **2010**, 48, 3033.

31. P. Ghosh, T. Soga, K. Ghosh, R. A. Afre, T. Jimbo, Y. Ando, J. Non Cryst. Solids. **2008**, 354, 4101

32. J. Liu, S. Webster, D. L. Carroll, J. Phys. Chem., **2005**, 109, 15769.

33. E. Cruz-Silva, D. A. Cullen, L. Gu, J. M. Romo-Herrera, E. Muñoz-Sandoval, F. López-Urías, B. G. Sumpter, V. Meunier, J. C. Charlier, D. J. Smith, H. Terrones, M. Terrones, ACS Nano, **2008**, 2, 441.

34. C. J. Lee, S. C. Lyu, H. W. Kim, J. H. Lee, I. C. Cho, Chem. Phys. Lett., **2002**, 359, 115.

35. J. Liu, R. Czerw, D. L. Carroll, Mater. Res., **2005**, 20, 538.

36. E. J. Liang, P. Ding, H. R. Zhang, X. Y. Guo, Z. L. Du, Diamond Relat. Mater., **2004**, 13, 69.

37. M. Terrones, N. Grobert, H. Terrones, Carbon, **2002**, 40, 1665.

38. L. Ci, H. Zhu, B. Wei, J. Liang, C. Xu, D. Wu, Carbon, **1999**, 37, 1652.

# CHAPTER 4

## 4. CONCLUSIONS AND RECOMMENDATIONS

### 4.1 Conclusions

The aim of this study was to synthesize nitrogen doped carbon nanotubes (N-CNTs) using the floating catalyst chemical vapour deposition (CVD) method utilizing iron pentacarbonyl as the catalyst and acetonitrile as a nitrogen source. In this study the N-CNTs were successfully synthesized and fully studied by means of Raman spectroscopy, thermogravimetric analysis (TGA) and transmission electron microscopy (TEM) analyses. Two different procedures were used to add the reagent to the reactor, an injection and a bubbling method. Most of the results for this study were achieved using the injection method. The influence of different parameters on the fabrication of N-CNTs was studied. These parameters include the physical parameters such as gas flow rate, growth temperature and the $Fe(CO)_5$/acetonitrile ratio. Their influence on the outer and inner diameters of N-CNTs, the size of bamboo compartment, yield, the thermal stability and crystallinity of the product were determined.

It was revealed that, the ratio of $Fe(CO)_5$/acetonitrile played a great role in determining the yield, morphology, crystallinity and thermal stability of the N-CNTs. It was observed from yield studies that an increase in acetonitrile concentration decreased the yield due to the role of nitrogen. The TEM studies showed that an increase in acetonitrile concentration decreased the outer diameters and as expected had no significant effect on the inner diameters. It was noticed that as the concentration of acetonitrile was increased, the distance between each bamboo cap was reduced. Further, when a solution contained 15% acetonitrile was used the tubes showed predominantly bamboo compartments. The thermal stability of the samples was analysed by TGA analysis and it was confirmed that, as the incorporation of N in the CNTs increased the stability of the sample decreased. Raman spectroscopy did

not reveal the results which were consistent with other literature studies. An increase in level of disorder only was observed from samples produced from 2% and 25% of actonitrile were used. However, it was assumed that the disorder ratio increased as the concentration of acetonitrile went up even though no increase was observed in samples made with 5%, 15% and 20% acetonitrile concentrations.

Reaction temperature was found to be a key parameter in the fabrication of N-CNTs. The effect of four different growth temperatures were studied as the temperature was varied from 750 $^{o}$C to 900 $^{o}$C. TEM analysis revealed that at 750 and 800 $^{o}$C no tubes were synthesized and only fibers, agglomerates and nanobeads/pearls were observed. Good carbon products were achieved at 850 and 900 $^{o}$C, and it was noticed that more tubes were formed at 850 $^{o}$C compared to 900 $^{o}$C.

The effect of temperature on the outer diameter distribution revealed that at both temperatures (850 $^{o}$C and 900 $^{o}$C) there was a wide range of tube outer diameters but the material synthesized at 850 $^{o}$C contained narrower tubes. No major temperature effect was observed on the average distance between the bamboo caps.

Some experiments were performed in which 5% hydrogen was added to an Ar atmosphere. It was reported in the literature [1] that $H_2$ can play an important role in changing the quality and quantity of CNT production. When hydrogen was added, it increased the yield of the product. It also reduced the amount of amorphous carbon since hydrogen reduced the rate of carbon production by hydrogenation to give more ordered and thermodynamically stable multi-walled carbon nanotubes (MWCNTs). Interestingly, it was observed that tubes with larger outer diameter were synthesized in the presence of hydrogen.

The bubbling method was applied to make a comparison between the injection and the bubbling approach to make CNTs. When both methods were compared in this study it was concluded that the bubbling method appeared as a more simple method to make better quality tubes. The yield however was very low.

## 4.2 Recommendations for future study

In this study $Fe(CO)_5$ was used as the catalyst and it created some problems due to its volatility. This included blockage of the tip of the injector. It is suggested for future study to use a solid compound as the catalyst viz $Fe(CO)_4CH_3CN$. This can be synthesized from a mixture of acetonitrile and $Fe(CO)_5$. This catalyst can be either used in solid form or be dissolved in a solvent. Another issue to be explored is the role of pressure on the reaction. The HiPco process is known to occur at pressure > 1 atmosphere. This may be an important parameter to make N-CNTs in high purity and yield.

## 4.3 References

1. V. O. Nyamori, S. D. Mhlanga, N. J. Coville, Organomet. Chem., **2008**, 693, 2205.